Genotoxic Impact of Aluminum-containing Nanomaterials in Human Intestinal and Hepatic Cells.

Pégah Jalili
Anses Laboratoire de Fougeres
Sylvie HUET
Anses Laboratoire de Fougeres
Agnès Burel
MRiC
Benjamin-Christoph Krause
Bundesinstitut fur Risikobewertung
Caroline Fontana
Institut National de Recherche et de Securite
Soizic Chevance
Institut des Sciences Chimiques de Rennes
Fabienne Gauffre
Institut des Sciences Chimiques de Rennes
Yves Guichard
Institut National de Recherche et de Securite
Alfonso Lampen
Bundesinstitut fur Risikobewertung
Peter Laux
Bundesinstitut fur Risikobewertung
Andreas Luch
Bundesinstitut fur Risikobewertung
Kevin Hogeveen
Anses Laboratoire de Fougeres
Valerie Fessard (Valerie.FESSARD@anses.fr)
Anses Laboratoire de Fougeres https://orcid.org/0000-0001-9046-9117

Research

Keywords: nanomaterials, comet assay, micronucleus, cell transformation assay, oxidative stress

Posted Date: September 16th, 2020

DOI: https://doi.org/10.21203/rs.3.rs-72845/v1

Version of Record: A version of this preprint was published at Toxicology in Vitro on October 1st, 2021.
See the published version at https://doi.org/10.1016/j.tiv.2021.105257.

Abstract

Background: Exposure of consumers to aluminum-containing nanomaterials (Al NMs) through numerous products is an area of concern for public health agencies since human health risks are not completely elucidated. In addition, the available data on the genotoxicity of Al_2O_3 and Al^0 NMs are inconclusive or rare. In order to provide further information, the present study investigated the *in vitro* genotoxic potential of Al^0 and Al_2O_3 NMs in intestinal and liver cell models since these tissues represent organs which would be in direct contact or could experience potential accumulation following oral exposure.

Methods: Differentiated human intestinal Caco-2 and hepatic HepaRG cells were exposed to Al^0 and Al_2O_3 NMs (0.03 to 80 µg/cm2) and the results were compared with those obtained with the ionic form $AlCl_3$. Several methods, including H2AX labelling, the alkaline comet assay and micronucleus (MN) assays were used. Oxidative stress and oxidative DNA damage were assessed using High Content Analysis (HCA) and the formamidopyrimidine DNA-glycosylase -modified comet assay respectively. Moreover, carcinogenic properties of Al NMs were investigated through the cell transforming assay (CTA) in Bhas 42 cells.

Results: The three forms of Al did not induce chromosomal damage when tested in the MN assay. Furthermore, no cell transformation was observed in Bhas 42 cells. However, although no production of oxidative stress was detected in HCA assays, Al_2O_3 NMs induced oxidative DNA damage in Caco-2 cells in the comet assay following a 24 h treatment. Considerable DNA damage was observed with Al^0 NMs in both cell lines in the comet assay, although this was likely due to interference with these NMs. Finally, no genotoxic effects were observed with $AlCl_3$.

Conclusion: The slight effects observed with Al NMs are therefore not likely to be related to ion release in the cell media.

1. Introduction

Within the last decade, aluminum (Al)-containing nanomaterials (NMs) have been widely used not only for industrial applications, but also in consumer products, due to their higher reactivity compared to the bulk form [1, 2, 3, 4]. Forms of Al, both in the micro-and the nano-size, are present in food and consumer products [1, 5] due to their use as firming, anticaking, neutralizing, emulsifying and texturizing agents, as well as for cooking tools [6], waste water treatment [7, 8] and in medical and hygiene products such as toothpaste [9, 10, 11]. Nevertheless, their potential toxicity has not been fully evaluated, leading to major concerns from consumers and public health agencies [12].

According to exposure estimates from the European Food Safety Authority (EFSA), consumers can absorb up to 2.3 mg Al /kg bw/week, more than twice the weekly tolerable intake (1 mg/kg bw/week) [7]. In addition, a recent study has estimated total consumer exposure to Al containing compounds, including

contributions from products used in food (additives, contact materials) and in cosmetics, and concluded that adolescents were highly exposed [13].

Few studies on the genotoxicity of nanoscale forms of Al following oral ingestion have been performed, and most of the published literature has focused on Al_2O_3 NMs only. DNA damage was reported in erythrocytes of rats after a single oral treatment with Al_2O_3 NMs, although at high doses (≥1,000 mg/kg) [14, 15]. Genotoxic effects were observed in bone marrow, but not in other organs, after a short-term treatement with lower doses of Al_2O_3 NMs [16]. *In vivo* effects of Al^0 NMs following oral exposure are mostly lacking, although one study suggested cross-linking effects on DNA in the duodenum of rats [16]. Following oral exposure of rodents with ionic forms of Al, an increase in MN frequency was reported in bone marrow after a single oral administration [17] and in liver after a 30 day oral treatment [18]. Nevertheless, the induction of MN formation in liver was shown to decrease with an antioxidant treatment [18, 19]. Consistent with these results, a slight oxidative DNA damage was observed in blood after a short-term oral exposure [16].

The *in vitro* genotoxicity of Al_2O_3 NMs has been assessed in several mammalian cell lines including human peripheral lymphocytes [20], primary human fibroblasts [21], hepatic HepG2 cells [22], and Chinese hamster ovary cells [23]. While some studies have not observed genotoxic effects of Al_2O_3 NMs [20, 24, 25, 26], others have reported a positive response [21, 22] which may be associated with oxidative damage [22]. In contrast, no data on the *in vitro* genotoxicity of Al^0 NMs has been published so far, and only some cytotoxicity was detected in rat alveolar macrophages treated with Al^0 above 100 µg/ml [27]. For the salt $AlCl_3$, DNA damage has been reported in human peripheral blood lymphocytes, with positive results in micronucleus and chromosomal aberration tests, as well as in the comet assay [17, 28, 29, 30].

According to an ECHA safety assessment [31], the data available on the genotoxicity of Al_2O_3 NMs are inconclusive while few data on the genotoxicity of Al^0 NMs has been published so far. In addition to the direct contact of Al NMs present in food with the intestinal epithelium, Al accumulation in liver has been shown after oral exposure with Al_2O_3 NMs [15, 32, 33].

Therefore, the aim of the current study was to evaluate the *in vitro* genotoxic potential of Al^0 and Al_2O_3 NMs in two relevant human cell models of intestine and liver. Several endpoints of genotoxicity were investigated using the alkaline and Fpg-modified comet assays which detects DNA breakage including oxidative lesions, DNA double strand breaks were detected through phosphorylated histone H2AX (γH2AX), and the micronucleus assay which determines chromosome and genome damage. Furthermore, the capacity of aluminum-containing NMs to initiate or promote carcinogenesis was assessed by the Cell Transforming Assay (CTA) in Bhas-42 cells.

As these NMs can potentially dissolve in the dispersion solution or in media, the genotoxicity was compared to that of the metal salt $AlCl_3$. Moreover, the interference of NMs, including with Al-NMs [34], has been demonstrated in numerous publications using a wide range of biological assays, and stresses

the necessity to evaluate interference in order to assess the potential effect on the results [35, 36, 37, 38]. In this study, various sources of interference have been taken into account within the different assays.

2. Materials And Methods

2.1 Chemicals and reagents

Dimethylsulfoxide (DMSO), insulin, cytochalasin B, formamidopyrimidine-DNA glycosylase (Fpg), trypan-blue, 12-*O*-tetradecanoylphorbol-13-acetate (TPA), 3-methylcholanthrene (3-MCA) and menadione (MEN) were supplied from Sigma (St. Quentin-Fallavier, France). Methylmethanesulfonate (MMS) was purchased by Acros Organics (Fairlawn, NJ). Dinophysistoxin-2 (DTX-2) was from the National Research Council Canada (NRCC, Ottawa, Canada). Penicillin, streptomycin, Williams' E medium and Fetal Bovine Serum Fetalclone II (FBS) were supplied from Invitrogen Corporation (Illkirch, France). For Bhas 42 cell cultures, Eagle's minimum essential medium and Dulbecco's modified Eagle's medium/Ham's F12 was from Invitrogen Corporation (Illkirch, France). Fetal bovine serum was obtained by Dutscher, (Brumath France). Hydrocortisone hemisuccinate, Hyclone^{TM} DMEM/high glucose and fetal bovine serum for Caco-2 cells were purchased from Upjohn Pharmacia (Guyancourt, France), GE Healthcare Life Science (Logan, UT, USA) and Capricorn scientific (Ebsdorfergrund, Germany), respectively. The primary and secondary antibodies (mouse monoclonal anti γH2AX ser139 (ab26350), rabbit monoclonal anti active caspase-3 antibody (ab13847), goat anti-rabbit IgG H&L AlexaFluor 647 (ab150079) and goat anti-mouse IgG H&L AlexaFluor 647 (ab150115)) were provided from Abcam (Cambridge, UK). CellROX® Deep Red Reagent was obtained from Invitrogen (Paisley, UK). Formaldehyde and Giemsa were purchased by Fisher (Illkirch-Graffenstaden, France).

2.2 Dispersion and characterization of NMs

Al^0, Al_2O_3 and ZnO NMs with a similar primary particle size were supplied from IoLiTec (Heilbronn, Germany). NM characteristics as provided by the supplier are presented in Table 1. $AlCl_3$ (hexahydrate) was purchased from Sigma Aldrich (Saint Louis, USA). NM dispersion was performed according to the NANOGENOTOX protocol [39], as described in [16].

The morphology and agglomeration of Al^0 and Al_2O_3 NMs in the stock dispersion solution and in cell media were determined by transmission electron microscopy (TEM) (Figure S 1). For the characterization of NMs from stock solutions, TEM grids were prepared immediately after sonication and dilution (100 µg/mL) in the stock dispersion solution. For the characterization of NMs in cell culture media (DMEM +10% FBS and William's Medium +5% FBS), the samples were diluted with distilled water to 1.2 µg/mL prior to grid preparation. The TEM grids were prepared by deposition of a carbon-coated copper grid onto a drop of the stock solution for 20 s to allow adsorption of the NMs and were observed with an electron microscope (JEOL 1400 operated at 120 kV and coupled with a 2k-2k camera from Gatan (Orius 1000)).

The hydrodynamic diameter of Al^0 and Al_2O_3 NMs were measured using a Malvern Zetasizer (Malvern Instruments, Malvern, UK) equipped with a 633-nm laser diode operating at an angle of 173°. To assess the stability of NM suspensions, following NM dispersion, samples were diluted to a final concentration of 100 µg/ml in the stock dispersion solution or in cell media and measurements were performed at 0 and 24 h. The samples were equilibrated at 25 °C for 120 s prior to measurement. Ten repeated measurements for each sample were performed in 3 independent experiments. The mean hydrodynamic diameter Z_{ave} was determined using cumulant analysis.

2.3 Cell culture and treatment

The human colorectal adenocarcinoma Caco-2 cell line was cultured (passages 25–38) until differentiation after 21 days as described in [40] including for cell seeding in various plate formats depending on the assay performed. Simarly, HepaRG cells (passages 13-19) were cultured and seeded for the various assays as previously described [40, 41].

Differentiated Caco-2 and HepaRG cells were treated for 24 h with Al^0 and Al_2O_3 NMs at concentrations ranging from 0.03 to 80 µg/cm^2 and with $AlCl_3$ as ionic salt control at 90 and 128 µg.mL^{-1} in DMEM + 10% FBS or William's medium + 5% FBS respectively. For some assays, ZnO NMs at concentrations from 1.5 to 6 µg/cm^2 were used as a positive NM control. Equivalence between volume concentration (µg/mL) and surface concentration (µg/cm^2) are shown in Table S 1B. Al content corresponding to the concentrations of Al-containing NMs and $AlCl_3$ that were used are summarized in Table S 1B.

2.4 Kinetics of nanoparticle sedimentation

The colloidal characterization of the suspended nanomaterials in the conditions of cellular uptake assay was achieved using the volumetric sedimentation method (VCM) as reported in DeLoid et al [42]. We first measured the volume of the potentially agglomerated NM in DMEM and Williams media, at a NM concentration of 250 µg.mL^{-1}, using a specific centrifugal tube and ruler device. From the measured pellet, the effective density (ρ_{eff}) is calculated using the following equation:

$$\rho_{eff} = \rho_m + \left[\left(\frac{M_{NP}}{V \times SF}\right)\left(1 - \frac{\rho_m}{\rho_{NP}}\right)\right]$$

Where ρ_m is the density of the medium in g.cm^{-3}, ρ_{NP} is the density of NP (2.7 g.cm^{-3} for Al and 3.95 for Al_2O_3), M_{NP} the total mass of NM in 1 mL of dispended volume and V the measured volume pellet. SF is a stacking factor and was set to 0.634, which generally is appropriate for random stacking. The loss of mass of NMs from ion release was estimated to be lower than 1% and was neglected in the density calculation. The viscosity of the cell culture media at 37°C was determined using a Nanoparticle Tracking

Analysis device (Malvern Instrument) by measuring the apparent hydrodynamic radius of 400 nm standard particles in the media. Finally, the kinetics of sedimentation was calculated using the distorded grid (DG) model available from DeLoid et al [42]. The size of the NPS was taken from Table 2 (Z_{ave}). Other model parameters are h=3.1mm (liquid column height), initial NM concentration : 0.250 $mg.mL^{-1}$, the dissolution and cell-NMs stickiness are neglected (parameters set to 0).

2.5 Ion release from NMs

Following the dispersion of Al^0 and Al_2O_3 NMs, suspensions were diluted in stock solution (ultra pure water + 0.05 % BSA) or cell culture media (DMEM +10% FBS and William's Medium +5% FBS) at concentrations of 25, 50 and 100 µg/mL. After 24 h, ion release from NMs was determined by ultracentrifugation at 16,000 g for 1 h at 4°C (Hettich Zentrifuge Mikro 220R). The supernatants were processed through acidic hydrolysis (69% HNO_3, 180°C for 20 min in an MLS-ETHOS Microwave system) before detection of Al species with a quadrupole Inductively Coupled Plasma Mass Spectrometry (ICP-MS) (iCAP Q, Thermo Fisher Scientific GmbH, Dreieich, Germany) equipped with a PFA ST Nebulizer, a quartz cyclonic spray chamber and a 2.5 mm quartz injector (Thermo Fisher Scientific). The gas flows were set to 14 L/min, and 0.65 L/min for the cool gas (Ar) and the auxiliary gas (Ar) respectively. The flow rate of the sample was 0.39 mL/min. Results are given as percentage of the initial Al amount.

2.6 Uptake observations by TEM

Following a 24 h treatment, cells were fixed by glutaraldehyde (2.5%) and embedded in DMP30-epon before cutting ultra-thin sections (90 nm) for TEM observation as described in [40].

2.7 Cellular imaging and High Content Analysis (HCA)

After 24 h treatment with Al NMs and $AlCl_3$, plates were processed for HCA with an ArrayScan VTI HCS Reader (Thermo Scientific, Waltham, USA) as described in [40]. Cell numbers were determined from DAPI staining, active caspase-3 was quantified in the total cell compartment and H2AX in cell nuclei.

Oxidative stress was measured using CellROX Deep Red Reagent (Fisher Scientific, Illkirch, France). Briefly, cells were pre-incubated for 1 h with 5 M CellROX in serum-free media and washed twice with PBS before treatment with NMs and $AlCl_3$. After 24 h and twice washing with PBS, cells were incubated with 3 M Hoescht 33342 for 20 min at 37°C. Cells were then washed twice with PBS and were scanned and analyzed using the Compartimental Analysis module of the Bioapplication software. For each well, images from 7 fields (20 × magnification) were analyzed for quantification of fluorescence at 647 nm.

2.8 Comet assay

After a 5 h (Figure S 3) or 24 h treatment with Al NMs and $AlCl_3$, the comet assay was performed as described in [40, 43]. The individual tail intensity of at least 50 cells per slide were analyzed using the Comet Assay IV software (Perceptive Instruments, Haverhill, UK). Cells were considered as hedgehogs when DNA damage was too high to score. At least three independent experiments were performed. Methyl methanesulfonate (MMS) was used as positive control.

The level of oxidized bases was determined with the modified comet assay using the bacterial DNA repair enzyme Fpg through the formation of single-strand breaks (SSB) induced by the excision of oxidized purines [44, 45]. Some additional steps to the protocol described above were performed such as incubation with enzyme buffer (0.1 M KCl, 0.2 mM EDTA, 40 mM HEPES, 0.2 mg/ml BSA) after lysis. Two slides, one incubated with enzyme buffer (control slide) and the other with 9 U/slide Fpg at 37°C for 30 min, were then processed as described previously.

2.9 Particle interaction with DNA during the comet assay

The interaction of NMs with DNA migration during the comet assay was evaluated as described previously [35, 40]. Briefly, dilutions of Al^0 or Al_2O_3 NMs in 0.5% low-melting point agarose (LMP) were prepared at final concentrations of 28 and 128 µg/mL (corresponding to 9 and 40 µg/cm^2 conditions). After trypsinization and centrifugation (2 min, 136 g), untreated Caco-2 and HepaRG cells were resuspended in the LMP/NM mixture, loaded on pre-coated slides and processed in the alkaline comet assay as previously described, in the presence or absence of Fpg. A negative control consisting of untreated cells in LMP-agarose in the absence of NMs was performed in order to compare the results.

2.10 Cytokinesis-block micronucleus assay (CBMN)

The CBMN assay was performed as described in [40] according to the guideline n°487 of the Organization for Economic Co-operation and Development (OECD) [46]. After staining of the slides with acridine orange (100 µg/mL), at least 1000 binucleated cells per slide were scored. Three independent experiments were carried outand each concentration was tested in duplicate. The replication index (RI) was calculated using the formula recommended by OCDE guideline n°487. MMS and ZnO NM were used as positive controls.

2.11 Bhas 42 Cell Transformation Assay (CTA)

Originally established from the v-Ha-ras-transfected BALB/c 3T3 cells by Sasaki et al [47], Bhas 42 cells used in this study (passage 23) were obtained from Harlan Laboratories (Rossdorf, Germany). Both the CTA and concurrent cell growth assays were performed in their 6-well format and in accordance with a

guidance document produced by the OECD [48], with some modifications. The protocol, including both an initiation and a promotion assay, was previously described by Fontana et al [49].

In the initiation assay, 24 h after seeding (420 cells/cm^2) (Day 1), the cells were treated with Al NMs and $AlCl_3$ for 72 h (Day 4). Then, the cells were cultivated in fresh medium until Day 21, with medium changes on Day 7, Day 10 and Day 14. MCA (1 µg/mL) was used as positive control.

In the promotion assay, the cells were seeded (1,500 cells/cm^2) and cultured for 4 days without changing the media. On Day 4, 7, and 10, the culture medium was replaced with fresh media containing Al NMs or $AlCl_3$. The treatment continued until Day 14. The cells were then cultured in fresh medium in the absence of NMs until Day 21. TPA (0.05 µg/mL) was used as positive control.

In both assays, the cells were fixed with ethanol on Day 21 and stained with a 5 % Giemsa solution. The morphological criteria recommended by OECD were followed for the evaluation of transformed foci. The mean of the number of transformed foci was calculated from six replicate wells.

Cell growth assays in both the initiation and promotion conditions were performed on Day 7 using three replicate wells for each condition. The cells were fixed in 4% formaldehyde and stained with 1 µg/mL DAPI. The number of cell in wells was determined by automated microscopy with an Arrayscan VTi using the Target Activation module of the BioApplication software. The relative cell growth (%) was calculated as follows: (number of cells in treated cultures / number of cell in control cultures) x100.

2.12 Statistical analysis

The statistical significance of HCA results was tested using one-way Analysis of variance (ANOVA) followed by Dunnett's post-hoc tests with GraphPad Prism 5.

For the comet assay, the one-way Analysis of variance (ANOVA) was used followed by Dunnett's post-hoc test.

For the micronucleus assay, the percentages of micronucleated cells in treated and solvent control cultures were compared using the one-way Pearson chi-square test.

For the CTA, data were statistically analysed by multiple comparison using the one-sided Dunnett's test ($p<0.05$, upper-sided). The significance of the positive controls (MCA and TPA) was evaluated relative to the control ($p < 0.05$) by the one-sided Student's t-test.

3. Results

3.1 Nanomaterial characterization

Information concerning the physico-chemical characterization, including the morphology, primary size, surface specific area (SSA), purity and density of the Al^0, Al_2O_3 and ZnO NMs used in this study are provided in Table 1. However, in contrast to the information provided by the suppliers, the particle morphology of Al_2O_3 NMs in the stock dispersion solution cannot be considered as being spherical, but rather have a rod-like shape when observed by TEM (Figure S1). Although Al^0 particles exhibit a spherical shape, numerous elongated protrusions are also observed (Figure S1). Therefore, values of "average particle size" (Table 1) should then be considered with caution. Due to the drying step for preparation of TEM grids, the crystallization of different components of the culture media did not allow a proper characterization of the morphology of Al NMs in cell culture media (data not shown).

Particle hydrodynamic diameter and stability in the stock dispersion solution, as well as in cell media, were assessed by DLS immediately (0 h), as well as after 24 h (Table 2). The hydrodynamic diameters of Al^0, Al_2O_3 and ZnO NMs in the dispersion stock solution were 254 ± 4 nm for Al^0, 168 ± 3 nm for Al_2O_3 and 233 ± 11 nm for ZnO immediately following dispersion and were stable over time. The stability over time of these NMs was also observed in cell media (Table 2). Nevertheless, the average hydrodynamic size of Al^0 and Al_2O_3 NMs were lower in DMEM + 10% FBS at any time of measurement compared to stock solution and William's media + 5% FBS medium. The average hydrodynamic size of ZnO NMs was similar in the stock dispersion solution and in the two media. Globally, although estimated to have a similar primary size, the average hydrodynamic sizes of Al_2O_3 NMs are consistently smaller than those measured for Al^0 and ZnO NMs.

The polydispersity index (PdI) of Al^0, Al_2O_3 and ZnO NMs suspensions in stock dispersion solution and in media were stable over time. Whereas the PdI was quite low (< 0.25) for all NMs in stock dispersion solution, it increased in cell media for Al_2O_3 (0.52 ± 0.027 in DMEM and 0.47 ± 0.015 in William's at 0 h) as well as for ZnO (0.27 ± 0.010 in DMEM and 0.23 ± 0.030 in William's at 0 h). This effect of media on the PdI was not observed for Al^0 NMs.

The sedimentation of particles during *in vitro* exposure is critical when considering interactions of cells with NMs. Indeed, in a typical experiment the NMs are dispensed onto adherent cells in well plates. Therefore the amount of particles in contact with cells depends on the rate of sedimentation. We applied the dosimetry method reported by DeLoid et al [42] to evaluate the sedimentation of Al^0 and Al_2O_3 NMs in DMEM and Willam's media in the conditions of cell exposure. When dispersed in culture medium, NMs may form agglomerates with adsorbed proteins and entrapped fluid. The effective density (ρ_{eff}) of these agglomerates should first be measured to determine the colloidal behavior of such agglomerates. The effective densities determined for Al^0 NMs are 1.18 and 1.19 in DMEM and William's media respectively. Densities of 1.24 and 1.17 were obtained for Al_2O_3 NMs in DMEM and William's cell culture media respectively. Applying the sedimentation model provided in DeLoid et al [42], we calculated the evolution of the concentration of NMs at the surface of cells with respect to time (Figure 1). The sedimentation of Al^0 NMs was similar in both media, and after 24 h the concentration at the bottom of the well is

approximately 650 µg/mL. The rate of sedimentation of Al_2O_3 NMs was relatively slower, and the difference was significantly more pronounced in William's medium, with a deposited concentration of 450 µg/mL at the bottom of the well after 24 h.

3.2 Ion release in stock solution and cell culture media

Ion release from Al NMs was investigated using ICP-MS (Table 3) and results are presented as percentages with respect to the initial concentration of aluminum. A decrease in the percentage of ion release from Al^0 NMs was observed with increasing NMs concentrations in both the stock dispersion solution (1.30 % at 25 µg/mL and 0.48 % at 100 µg/mL) and in media (3.88 % to 0.95 % in DMEM, and 2.42 % to 0.68 % in William's for 25 and 100 µg/mL respectively). Nevertheless, ion release from Al^0 NMs was slightly higher in media when compared to the dispersion stock solution. A concentration-dependent decrease in ion release was also observed for ZnO NMs (Table 3). Ion release was also higher in media compared to dispersion stock solution.

In contrast to Al^0 and ZnO NMs, for Al_2O_3 NMs, the percentage of ion release with respect to the initial concentration was very low, relatively stable and independent of the NM concentration, although ion release was slightly higher in cell media.

The level of ions from $AlCl_3$ solutions was stable and independent of the concentration in the stock solution, but decreased with increasing concentration in media. This decrease of ion concentration with higher concentrations is likely due to the precipitate formed by $AlCl_3$ in cell media.

3.3 Uptake of Al NMs in Caco-2 and HepaRG cells

The uptake and the intracellular distribution of Al^0 and Al_2O_3 NMs following a 24 h treatment in Caco-2 and HepaRG cells were investigated by TEM (Figure 2 and 3). In both cell lines, the majority of Al^0 NMs were found as dense agglomerates of various sizes in the cytoplasm embedded in electron lucent or dense vesicles which are likely endosomes and lysosomes (Figure 2 and 3, B and C, notched arrows). Moreover, in certain cases, some Al^0 NMs were observed as isolated nanoparticle clusters in the cytoplasm proximal to the nucleus (Figure 2 and 3 C, full arrows). Observations of Al^0 NMs in the nucleus were very rare, and this result requires further investigation as it may be due to artefacts. The distribution pattern observed for Al_2O_3 NMs was similar in both cell lines. While a perinuclear localization of Al_2O_3 NMs was also seen, this occured less frequently than for Al^0 NMs (Figure 2 and 3, D and E). Even at the lowest concentration, Al^0 and Al_2O_3 NMs were internalized through vesicle formation, most likely endocytosis, and accumulated in the cytoplasm of Caco-2 and HepaRG cells (Figure S 2).

3.4 Cytotoxicity

Viability and apoptosis in Caco-2 and HepaRG cells following a 24 h treatment with Al NMs were investigated by cell counts (Figure 4 A) and active caspase-3 labeling (Figure 4 B) respectively using automated image analysis. No significant change in cell numbers and active caspase-3 levels were observed in either Caco-2 or HepaRG cells treated with Al^0 and Al_2O_3 NMs up to 80 µg/cm^2. In addition, no significant cytotoxic effects were observed in cells treated with the ionic salt control $AlCl_3$ up to 128 µg/mL Al content (1.16 mg/mL $AlCl_3$).

Similarly, no significant change in cell numbers were observed in Caco-2 cells treated with ZnO at the concentrations tested. However, a significant decrease in cell numbers as well as an increase in active caspase-3 levels was observed for the highest dose (6 µg/cm^2) of ZnO NMs in HepaRG cells.

3.5 Oxidative stress

Quantification of intracellular ROS was used to evaluate oxidative stress in Caco-2 and HepaRG cells following a 24 h treatment (Figure 5). Intracellular reactive oxygen species (ROS) levels were not significantly changed following treatment up to 80 µg/cm^2 with Al^0 and Al_2O_3 NMs or the ionic salt control $AlCl_3$. However, treatment with ZnO NMs significantly increased levels of ROS at the highest concentration (6 µg/cm^2) in HepaRG cells.

3.6 Genotoxicity

3.6.1 γH2AX

Quantification of γH2AX labeling was used to evaluate the induction of DNA double stand breaks in Caco-2 and HepaRG cells following a 24 h treatment with Al NMs. Compared to untreated cells, the γH2AX levels were not affected in the nuclei of Caco-2 cells treated for 24 h with Al^0 and Al_2O_3 NMs up to 80 µg/cm^2, with ZnO NMs, or with the ionic salt control $AlCl_3$ up to 128 µg/mL (Figure 6). However in HepaRG cells, Al^0 NMs induced a slight but statistically significant increase in γH2AX levels at the highest concentration (80 µg/cm^2) tested. ZnO NMs induced significant increases at 3 and 6 µg/cm^2.

3.6.2 Comet assay

The potential for Al^0 and Al_2O_3 NMs to induce DNA damage in Caco-2 and HepaRG cells was investigated with the alkaline comet assay after a 24 h treatment (Figure 7 A and B). A modified comet assay with the Fpg enzyme was also performed to detect oxidative DNA damage (Figure 7 C and D).

In Caco-2 cells, a significant increase in tail DNA was observed with Al^0 NMs from 28 to 80 µg/cm^2 in the alkaline comet assay (Figure 7 A). In contrast, neither Al_2O_3 and ZnO NMs, or the ionic salt control $AlCl_3$ induced any significant increase in tail DNA. In the Fpg-modified comet assay, a significant increase in tail DNA was observed in cells treated with Al_2O_3 NMs at 3, 9 and 80 µg/cm^2 (Figure 7 C).

In HepaRG cells, tail DNA significantly increased in a dose-dependent manner in cells treated with Al^0 NMs, including a very considerable effect starting at 28 µg/cm^2. In contrast, no effect was observed for cells treated with Al_2O_3 and ZnO NMs, or the ionic control $AlCl_3$ (Figure 7 B). Similarly, an increase in tail DNA in the Fpg-modified comet assay was observed for Al^0 NMs at all concentrations tested with a very significant effect observed at concentrations above 9 µg/cm^2. No significant changes in tail DNA were detected in HepaRG cells treated with Al_2O_3 and ZnO NMs or $AlCl_3$ (Figure 7 D).

DNA damage in Caco-2 and HepaRG was also investigated by the alkaline comet assay after a 5 h treatment (Figure S 3). In Caco-2 cells, a concentration-dependent increase in tail DNA was observed in cells treated with Al^0 NMs from 28 to 80 µg/cm^2. No effect was detected in cells treated with Al_2O_3 and ZnO NMs, or the ionic salt control $AlCl_3$. In HepaRG cells, a concentration-dependent increase was also observed with Al^0 NMs from 9 to 80 µg/cm^2. In the Fpg-modified comet assay, an increase in tail DNA was detected in Caco-2 cells treated with Al^0 NMs from 9 to 80 µg/cm^2 and with Al_2O_3 NMs at 3, 9 and 28 µg/cm^2. Interestingly, in HepaRG cells treated for 5 h with Al NMs, results from the Fpg-modified comet assay showed that at every concentration tested, only hedgehogs were observed for all NMs (data not shown).

3.6.3 Interaction of NMs with DNA during the comet assay

The interference of NMs with the comet assay was assessed (Figure 8) according to the protocol described by Bessa et al [35]. Compared to the untreated control, a concentration-dependent increase in % tail DNA was observed when Al^0 NMs are added at final concentrations of 9 and 40 µg/cm^2. A similar effect was also observed when Fpg was included in the assay. Compared to the negative control, no difference was detected for Al_2O_3 NMs in the absence of Fpg, while a slight increase was observed with Fpg.

3.6.4 Micronucleus assay

In order to evaluate chromosome damage, the cytokinesis-block micronucleus assay was performed in Caco-2 and HepaRG cells treated for 24 h (Table 4) with Al NMs. No modification of cell viability (RI value) was observed in either Caco-2 or HepaRG cells exposed to Al^0, Al_2O_3, ZnO NMs and $AlCl_3$. Compared to the negative control, no significant increase in the percentage of BNMN cells was detected

in either cell line. Similarly, no increase in micronucleated mononuleated cells or in polyploid cells was observed (data not shown).

4. Bhas-42 Cell transforming (CTA) assay

Results of Bhas-42 CTA performed with Al^0 and Al_2O_3 NMs and with $AlC1_3$ are shown in Table 5. In the initiation assay, both Al^0 NMs and $AlC1_3$ induced a concentration-dependent decrease in cell proliferation on Day 7, inhibiting around 90% of cell proliferation at the highest concentration (3 µg/cm^2 for Al^0 NMs and 28 µg/ml for $AlCl_3$). In contrast, Al_2O_3 NMs in the initiation assay and the three Al forms in the promotion assay induced no, or only a moderate, decrease in cell proliferation for all concentrations tested. No transforming activity was shown with the three Al forms, irrespective of the concentration tested in both the initiation and promotion assays. In contrast, the number of foci was found lower than those of controls at some concentrations of Al and Al_2O_3.

4. Discussion

Exposure of the general population to NMs present in consumer products, including food, has increased dramatically within the last decade, and a thorough evaluation of the potential adverse effects resulting from exposure to NMs following ingestion is necessary. Among the toxic effects of Al-containing NMs that have been shown in several studies, genetic damage is of particular concern [15, 21, 22, 23]. Both intestine and liver are considered key organs for investigating genotoxic effect of nanomaterials found in food since they represent the main organ of contact and the main organ of accumulation, respectively. Nevertheless, in our recent *in vivo* study investigating the genotoxicity of Al NMs, only a very limited genotoxic response was observed. In fact, only a cross-linking effect was suggested in the rat duodenum with Al^0 NMs [16]. As the *in vivo* treatment duration was rather short (3 administrations over 2 days), and that it cannot be excluded that the level of NMs in the organs would be low, we chose to complete our study by investigating the *in vitro* genotoxicity of Al NMs in human intestinal Caco-2 and hepatic HepaRG cells using complementary tests.

Despite the uptake and presence of Al NMs in Caco-2 and HepaRG cells, no cytotoxicity or apoptotic response was observed following treatment with Al_2O_3 NMs. Our results are in agreement with data from various publications that have reported little or no cytotoxicity in various cell lines [21, 27, 34, 50, 51], including in Caco-2 cells [52, 53] and HepG2 cells [22].

No induction of chromosomal damage was observed in the micronucleus assay in either Caco-2 or HepaRG cells exposed to Al_2O_3 NMs. Moreover, we did not observe a transforming activity in the CBA assay, supporting the absence of mutagenic potential for Al_2O_3 NMs. Our results are consistent with two recent studies that reported a negative response in the chromosomal aberration and the micronucleus assays in human lymphocytes treated with Al_2O_3 NMs with a smaller size (3 to 4 nm) than the one used in this study (20 nm), and for a longer incubation time (72 h) [20, 54]. In contrast, other studies have

reported an increase in micronucleus formation following a 24 h treatment with Al_2O_3 NMs in other cell lines, including CHO cells [23], human fibroblasts [21] and RAW264 murine macrophages [24]. Interestingly, Al_2O_3 NMs were shown to inhibit the replication efficiency of high-fidelity DNA polymerase [55]. Nevertheless, such inhibition did not affect the mutation rate at the single nucleotide level of replication products compared to controls [55]. Further investigation demonstrated that Al_2O_3 NMs did not induce a clastogenic effect but rather chromosome loss and polyploidy, although these effects were observed only at one concentration [21]. An aneugenic effect of Al NMs was not observed in our study (data not shown). The discrepancy may be explained by the fact that our tests were performed in non-proliferating cells.

Similarly, numerical chromosomal damage (aneuploidy and polyploidy) and abnormal metaphases were reported in the bone marrow of rats 48 hours after a single oral dose of Al_2O_3 NMs while no effect was observed with bulk Al_2O_3 [14, 15]. In addition, induction of micronuclei in erythrocytes was also observed. However, this genotoxic effect on erythrocytes was concomitant with a cytotoxic effect, while no toxicity was observed in our study [16], or in the study of Zhang et al [56]. In contrast, other results obtained from *in vivo* studies are in agreement with the lack of chromosomal damage observed *in vitro* in our study following treatment with Al_2O_3 NMs. In fact, with the same Al_2O_3 NMs used in this study, we did not observe an induction of micronuclei in either bone marrow or in the colon of rats after a short-term oral treatment [16]. Similarly, no induction of micronuclei in the bone marrow of mice was detected following intraperitoneal injections, irrespective of the size of the Al_2O_3 particles [56].

The absence of genotoxic activity of Al_2O_3 NMs in Caco-2 and HepaRG cells was further confirmed in the H2AX assay as well as the comet assay. We did not observe any increase in H2AX levels in either cell line, which is in agreement with results from a study by Tsaousi et al [21] in primary human fibroblasts. Additionally, Al_2O_3 NMs did not induce DNA damage in the alkaline comet assay in Caco-2 and HepaRG cells following a 24 h treatment. Although some studies have reported negative results in the comet assay in human lymphocytes and in human embryonic kidney cells [20, 26], others have demonstrated time- and/or concentration-dependent genotoxic effects in Chinese hamster lung fibroblasts [56], in RAW264 murine macrophages [24] and in human liver HepG2 cells [22] treated with Al_2O_3 NMs. Nevertheless, the increase of DNA fragmentation in these latter studies was probably linked to cell death detected by Trypan blue exclusion [56] or by apoptotic markers [22, 24].

In vivo, after a short-term treatment using the same Al_2O_3 NMs, we only observed an increase in DNA damage in the comet assay in bone marrow, while no effect was observed in intestine, colon, kidney, spleen or blood [16]. Balasubramanyam et al [14] showed a time- and concentration-dependent increase in DNA damage in blood with the comet assay with both bulk and nano Al_2O_3 forms after a single gavage but the effect decreased at 48 h before disappearing at 72 h. DNA breakage associated with necrosis and apoptosis was observed in liver and kidney of rats after a repeated oral treatment for 75 days with 70 mg/kg bw Al_2O_3 NMs [57]. Therefore, it seems that both the *in vitro* and *in vivo* results with Al_2O_3 NMs

support the conclusion that DNA breaks detected by the comet assay were mostly related to cell death rather than to a clear genotoxicity.

Nevertheless, we have shown that Al_2O_3 NMs induced oxidative DNA damage in Caco-2 cells following a 24 h treatment, despite no significant ROS induction. Furthermore, a concentration-dependent trend towards oxidative damage was observed at 5 h. This could suggest the rapid formation of oxidative DNA damage which is further repaired, as previously demonstrated [58, 59]. Evidence from *in vitro* experiments in a variety of different cell lines suggests that treatment with Al_2O_3 NMs can induce oxidative stress [20, 56, 60, 61] including in Caco2 cells [53]. Interestingly, Alarifi et al [22] reported positive results in the comet assay in HepG2 cells which was accompanied by oxidative damage and cell death. In the present study, no oxidative DNA damage or oxidative stress was observed in HepaRG cells. Differentiated HepaRG cells represent a model which is more similar to human hepatocytes when compared to HepG2 cells, and could therefore be less sensitive to oxidative damage resulting from Al_2O_3 NMs. Similarly, we did not detect oxidative DNA damage in liver, or in other organs of rats after oral exposure [16]. In contrast, an increase in oxidative stress was observed in several tissues including liver after acute and repeated oral exposure of rats with Al_2O_3 NMs [33].

Similar to the results obtained for Al_2O_3 NMs, no cytotoxicity or apoptotic response was observed following treatment with Al^0 NMs, despite their presence in the cytoplasm of Caco-2 and HepaRG cells. In contrast to our results in differentiated Caco-2 and HepaRG cells, Al^0 NMs were found to induce a decrease in viability in rat alveolar macrophages and in BRL3A rat liver cells following 24 h exposure at concentrations similar to those used in our study [27, 62]. This discrepancy could be explained by a difference in relative cell density for a similar concentration of Al^0 NMs tested with a lower NM:cell ratio in differentiated Caco2 and HepaRG cells compared to the two other proliferating cell systems.

Despite only a slight increase in H2AX levels observed only in HepaRG cells and only at the highest concentration tested, a dose-dependent increase in tail DNA was observed in both Caco-2 and HepaRG cell lines treated with Al^0 NMs using the alkaline comet assay after both 5 h and 24 h treatments. Nevertheless, this result required further investigation due to possible interference of NMs with the alkaline comet assay that has been widely documented in the literature [35, 36, 63, 64]. Indeed, NMs present in the cytoplasm of cells following uptake can interact with DNA following the lysis step of the comet assay, and could therefore induce additional breaks or inhibit DNA migration. In addition, a dissolution due to the conditions of the comet assay could result in reaction of aluminum ions with DNA, especially the phosphate backbone, as reported in some studies [65, 66]. Such reactions may then induce DNA damage revealed during the comet assay as suggested by Zhang et al [67]. Our results clearly demonstrate that, unlike Al_2O_3 NMs, Al^0 NMs can induce DNA damage when in contact with DNA and interfere significantly with the comet assay. Consequently, the positive results in cells treated with Al^0 NMs obtained in this study should therefore be treated with caution. *In vivo*, using the same Al^0 NMs as the present study, no genotoxic response was observed in several key tissues, with the exception in rat duodenum where a cross-linking effect was suggested [16].

The carcinogenic potential of Al NMs was investigated using the cell transformation assay with Bhas 42 cells. Neither Al^0 nor Al_2O_3 NMs induced cell transformation, although a decrease in the number of transformed foci was observed. This decrease, observed at concentrations inducing a weak inhibition of cell proliferation at Day 7, is likely explained by a more pronounced inhibition of cell growth after 21 days of culture due to the three repeated treatments during the promotion assay. This phenomena was also observed with amorphous silica NMs [49] as well as with other non-carcinogenic chemicals such as L-ascorbic acid and caffeine [68].

Ion release from NMs in cell culture media, or in intracellular compartments can contribute to cytotoxic effects *in vitro*. The soluble fraction of Al^0 and Al_2O_3 NMs measured by ICP-MS demonstrated a very low solubility of Al^0 and Al_2O_3 NMs in both cell media . However, ion release may occur after cell uptake in specific compartments with low pH such as lysosomes [69] as suggested for Al_2O_3 NMs [24]. In such a scenario, secondary effects affecting mitochondria and resulting in the generation of ROS cannot be excluded. In the case of Al^0, the formation of a passivating oxide layer may influence its dissolution behavior [70]. Consequently, effects could be induced by ionic Al released from the NMs rather than effects related to the particulate form [1]. As a strong oxygen acceptor, the Al ion tends to bind to citrate, phosphate, and catecholamine, generating oxygen radicals [1, 71]. In addition, Al ions can also bind to negatively charged phospholipids, which are easily attacked by reactive oxygen species such as $O_2^{\cdot}$, H_2O_2, and $OH^{\cdot}$ [72, 73] as well as DNA [66].

No genotoxic effects were observed in differentiated Caco-2 or HepaRG cells treated with $AlCl_3$ at concentrations up to 128 µg/mL Al content corresponding to 1.16 mg/mL $AlCl_3$. At the concentrations of $AlCl_3$ tested, no effects were observed in the different assays following 5 or 24 h treatments. Indeed, negative results were obtained for promotion and initiation, as well as for genotoxic and oxidative stress responses. Our results are consistent with Villarini et al [74] who observed no genotoxicity in response to Al ions in neuroblastoma cells with the comet assay, as well as no cytotoxicity or oxidative stress. However, other studies have reported genotoxicity of $AlCl_3$ in human lymphocytes [17, 29]. Interestingly, the authors of this study observed the highest level of micronuclei during the G1-phase of the cell cycle. The differentiated HepaRG and Caco2 cells used in our study are not proliferating, and therefore could explain the discrepancy between the studies. *In vitro*, chromosomal damage observed in blood cells at $AlCl_3$ concentrations below 25 µg/mL, was associated with apoptosis [28, 29, 30]. Moreover it was shown that Al ions can induce oxidative DNA damage irrespective of the cell cycle phase [29]. Indeed, the role of Al ions in mediating genotoxic effects may be more complex, as it has been suggested that Al ions may inhibit several DNA repair proteins with zinc finger domains [29, 75].

In our study, as the soluble fraction of $AlCl_3$ was always higher than that for Al^0 and Al_2O_3 NMs, the effects observed for Al^0 and Al_2O_3 NMs are not likely to be related to ion release in cell media. Although ECHA emphasized that the difference in the toxicological profile between soluble aluminum compounds and insoluble aluminum oxide may be explained by lower bioavailability of insoluble test compounds, it

was recently shown that the content of Al in blood of rats treated orally was higher with Al_2O_3 NMs than with $AlCl_3$ [76]. Moreover, the persistence of NMs in organs long after intial exposures has been described, and the accumulation of Al NMs in organs following repeated exposure could poteniate adverse effects in tissues in the long term. Further studies are clearly needed to investigate the fate of accumulated NMs in tissue, including possible effects due to ion release, as well as toxic effects related to particle accumulation.

5. Conclusion

In summary, despite the uptake and presence of Al NMs in the cytoplasm of differentiated Caco-2 and HepaRG cells, we have shown that Al_2O_3 NMs do not induce apoptosis, oxidative stress, or cytotoxic effects following a 24 h treatment. In addition, Al_2O_3 NMs were negative in the micronucleus assay, and in initiation and promotion in the CTA. Nevertheless, oxidative DNA damage was observed in Caco-2 cells. The assays performed with Al^0 NMs and $AlCl_3$ were also negative except a slight increase of H2AX levels only in HepaRG cells, and only at the highest concentration tested. Considerable DNA damage was observed with Al^0 NMs in both Caco-2 and HepaRG cells in the comet assay, although this was likely associated with the significant interference with these NMs, and these results must be taken with caution. As ion release from Al NMs was shown to be very limited in cell media, the effects are rather due to the particulate form or to ion release inside the cells. Further investigation is needed to clarify the extent of intracellular ion release from NMs, its contribution to cytotoxic effects compared to the direct impact of the presence of intracellular particles.

Declarations

Ethical Approval and Consent to participate

Not applicable.

Consent for publication

Not applicable.

Availability of supporting data

The datasets used and/or analysed during the current study are available from the corresponding author on reasonable request.

Competing interests

The authors declare that they have no competing interests.

Funding

This publication arises from the French-German bilateral project SolNanoTOX funded by the German Research Foundation (DFG, Project ID: DFG (FKZ LA 3411/1-1 respectively LA 1177/9-1) and the French National Research Agency (ANR, Project ID: ANR-13-IS10-0005).

Authors' contributions

PJ and AB performed the electron microscopy study and analysis. BCK performed the experiments for dispersion and dissolution characterization. CF and YG performed and analysed the CTA. FG and SC performed the density and dispersion chracterisation. PJ, SH and KH performed the genotoxicity experiments. PJ, BCK, FG, YG, KH and VF wrote the manuscript. AB, FG, AlL, PL, AnL, KH and VF wrote the proposal to obtain funding. All authors read and approved the final manuscript.

Acknowledgements

The authors would like to thank Rachelle Lanceleur and Marie-Thérèse Lavault for technical assistance.

References

1. Willhite CC, Karyakina NA, Yokel RA, Yenugadhati N, Wisniewski TM, Arnold IM, et al. Systematic review of potential health risks posed by pharmaceutical, occupational and consumer exposures to metallic and nanoscale aluminum, aluminum oxides, aluminum hydroxide and its soluble salts. Critical reviews in toxicology. 2014;44 Suppl 4:1-80; doi: 10.3109/10408444.2014.934439.
2. Som C, Wick P, Krug H, Nowack B. Environmental and health effects of nanomaterials in nanotextiles and façade coatings. Environment International. 2011;37 6:1131-42; doi: 10.1016/j.envint.2011.02.013.
3. Shepard MN, Brenner S. An Occupational Exposure Assessment for Engineered Nanoparticles Used in Semiconductor Fabrication. The Annals of Occupational Hygiene. 2013;58 2:251-65; doi: 10.1093/annhyg/met064.
4. Li X, Aldayel AM, Cui Z. Aluminum hydroxide nanoparticles show a stronger vaccine adjuvant activity than traditional aluminum hydroxide microparticles. J Control Release. 2014;173:148-57; doi: 10.1016/j.jconrel.2013.10.032.
5. Saiyed SM, Yokel RA. Aluminium content of some foods and food products in the USA, with aluminium food additives. Food additives and contaminants. 2005;22 3:234-44; doi: 10.1080/02652030500073584.

6. Moradi Z, Esmaiili M, Almasi H. Development and characterization of kefiran - Al2O3 nanocomposite films: Morphological, physical and mechanical properties. International Journal of Biological Macromolecules. 2019;122:603-9; doi: 10.1016/j.ijbiomac.2018.10.193.
7. European Food Safety A. Safety of aluminium from dietary intake - Scientific Opinion of the Panel on Food Additives, Flavourings, Processing Aids and Food Contact Materials (AFC). EFSA Journal. 2008;6 7:754; doi: 10.2903/j.efsa.2008.754.
8. Kumar E, Bhatnagar A, Kumar U, Sillanpää M. Defluoridation from aqueous solutions by nano-alumina: Characterization and sorption studies. Journal of Hazardous Materials. 2011;186 2:1042-9; doi: 10.1016/j.jhazmat.2010.11.102.
9. Zhang D, Quayle MJ, Petersson G, van Ommen JR, Folestad S. Atomic scale surface engineering of micro- to nano-sized pharmaceutical particles for drug delivery applications. Nanoscale. 2017;9 32:11410-7; doi: 10.1039/C7NR03261G.
10. Zhao J, Castranova V. Toxicology of nanomaterials used in nanomedicine. Journal of toxicology and environmental health Part B, Critical reviews. 2011;14 8:593-632; doi: 10.1080/10937404.2011.615113.
11. Narayan RJ, Adiga SP, Pellin MJ, Curtiss LA, Hryn AJ, Stafslien S, et al. Atomic layer deposition-based functionalization of materials for medical and environmental health applications. Philosophical transactions Series A, Mathematical, physical, and engineering sciences. 2010;368 1917:2033-64; doi: 10.1098/rsta.2010.0011.
12. Laux P, Tentschert J, Riebeling C, Braeuning A, Creutzenberg O, Epp A, et al. Nanomaterials: certain aspects of application, risk assessment and risk communication. Archives of toxicology. 2018;92 1:121-41; doi: 10.1007/s00204-017-2144-1.
13. Tietz T, Lenzner A, Kolbaum AE, Zellmer S, Riebeling C, Gürtler R, et al. Aggregated aluminium exposure: risk assessment for the general population. Archives of toxicology. 2019;93 12:3503-21; doi: 10.1007/s00204-019-02599-z.
14. Balasubramanyam A, Sailaja N, Mahboob M, Rahman MF, Hussain SM, Grover P. In vivo genotoxicity assessment of aluminium oxide nanomaterials in rat peripheral blood cells using the comet assay and micronucleus test. Mutagenesis. 2009;24 3:245-51; doi: 10.1093/mutage/gep003.
15. Balasubramanyam A, Sailaja N, Mahboob M, Rahman MF, Misra S, Hussain SM, et al. Evaluation of genotoxic effects of oral exposure to aluminum oxide nanomaterials in rat bone marrow. Mutation research. 2009;676 1-2:41-7; doi: 10.1016/j.mrgentox.2009.03.004.
16. Jalili P, Huet S, Lanceleur R, Jarry G, Le Hegarat L, Nesslany F, et al. Genotoxicity of Aluminum and Aluminum Oxide Nanomaterials in Rats Following Oral Exposure. Nanomaterials (Basel). 2020;10 2:305; doi: 10.3390/nano10020305.
17. Paz LNF, Moura LM, Feio DCA, Cardoso MdSG, Ximenes WLO, Montenegro RC, et al. Evaluation of in vivo and in vitro toxicological and genotoxic potential of aluminum chloride. Chemosphere. 2017;175:130-7; doi: 10.1016/j.chemosphere.2017.02.011.

18. Turkez H, Yousef MI, Geyikoglu F. Propolis prevents aluminium-induced genetic and hepatic damages in rat liver. Food and chemical toxicology : an international journal published for the British Industrial Biological Research Association. 2010;48 10:2741-6; doi: 10.1016/j.fct.2010.06.049.
19. Turkez H, Geyikoglu F, Tatar A. Borax counteracts genotoxicity of aluminum in rat liver. Toxicology and industrial health. 2013;29 9:775-9; doi: 10.1177/0748233712442739.
20. Rajiv S, Jerobin J, Saranya V, Nainawat M, Sharma A, Makwana P, et al. Comparative cytotoxicity and genotoxicity of cobalt (II, III) oxide, iron (III) oxide, silicon dioxide, and aluminum oxide nanoparticles on human lymphocytes in vitro. Human & experimental toxicology. 2016;35 2:170-83; doi: 10.1177/0960327115579208.
21. Tsaousi A, Jones E, Case CP. The in vitro genotoxicity of orthopaedic ceramic (Al2O3) and metal (CoCr alloy) particles. Mutation research. 2010;697 1-2:1-9; doi: 10.1016/j.mrgentox.2010.01.012.
22. Alarifi S, Ali D, Alkahtani S. Nanoalumina induces apoptosis by impairing antioxidant enzyme systems in human hepatocarcinoma cells. Int J Nanomedicine. 2015;10:3751-60; doi: 10.2147/IJN.S82050.
23. Di Virgilio AL, Reigosa M, Arnal PM, Fernández Lorenzo de Mele M. Comparative study of the cytotoxic and genotoxic effects of titanium oxide and aluminium oxide nanoparticles in Chinese hamster ovary (CHO-K1) cells. Journal of Hazardous Materials. 2010;177 1:711-8; doi: 10.1016/j.jhazmat.2009.12.089.
24. Hashimoto M, Imazato S. Cytotoxic and genotoxic characterization of aluminum and silicon oxide nanoparticles in macrophages. Dental Materials. 2015;31 5:556-64; doi: 10.1016/j.dental.2015.02.009.
25. McKenna DJ, Gallus M, McKeown SR, Downes CS, McKelvey-Martin VJ. Modification of the alkaline Comet assay to allow simultaneous evaluation of mitomycin C-induced DNA cross-link damage and repair of specific DNA sequences in RT4 cells. DNA Repair. 2003;2 8:879-90; doi: 10.1016/S1568-7864(03)00086-7.
26. Demir E, Burgucu D, Turna F, Aksakal S, Kaya B. Determination of TiO2, ZrO2, and Al2O3 nanoparticles on genotoxic responses in human peripheral blood lymphocytes and cultured embryonic kidney cells. Journal of toxicology and environmental health Part A. 2013;76 16:990-1002; doi: 10.1080/15287394.2013.830584.
27. Wagner AJ, Bleckmann CA, Murdock RC, Schrand AM, Schlager JJ, Hussain SM. Cellular Interaction of Different Forms of Aluminum Nanoparticles in Rat Alveolar Macrophages. The Journal of Physical Chemistry B. 2007;111 25:7353-9; doi: 10.1021/jp068938n.
28. Lima PDL, Leite DS, Vasconcellos MC, Cavalcanti BC, Santos RA, Costa-Lotufo LV, et al. Genotoxic effects of aluminum chloride in cultured human lymphocytes treated in different phases of cell cycle. Food and Chemical Toxicology. 2007;45 7:1154-9; doi: 10.1016/j.fct.2006.12.022.
29. Lankoff A, Banasik A, Duma A, Ochniak E, Lisowska H, Kuszewski T, et al. A comet assay study reveals that aluminium induces DNA damage and inhibits the repair of radiation-induced lesions in

human peripheral blood lymphocytes. Toxicology letters. 2006;161 1:27-36; doi: 10.1016/j.toxlet.2005.07.012.

30. Banasik A, Lankoff A, Piskulak A, Adamowska K, Lisowska H, Wojcik A. Aluminum-induced micronuclei and apoptosis in human peripheral-blood lymphocytes treated during different phases of the cell cycle. Environmental toxicology. 2005;20 4:402-6; doi: 10.1002/tox.20125.
31. ECHA. Registration dossier Aluminum oxide. https://echa.europa.eu/fr/registration-dossier/-/registered-dossier/16039/7/7/1.
32. Park EJ, Sim J, Kim Y, Han BS, Yoon C, Lee S, et al. A 13-week repeated-dose oral toxicity and bioaccumulation of aluminum oxide nanoparticles in mice. Archives of toxicology. 2015;89 3:371-9; doi: 10.1007/s00204-014-1256-0.
33. Shrivastava R, Raza S, Yadav A, Kushwaha P, Flora SJS. Effects of sub-acute exposure to TiO2, ZnO and Al2O3 nanoparticles on oxidative stress and histological changes in mouse liver and brain. Drug and Chemical Toxicology. 2014;37 3:336-47; doi: 10.3109/01480545.2013.866134.
34. Monteiro-Riviere NA, Oldenburg SJ, Inman AO. Interactions of aluminum nanoparticles with human epidermal keratinocytes. Journal of applied toxicology : JAT. 2010;30 3:276-85; doi: 10.1002/jat.1494.
35. Bessa MJ, Costa C, Reinosa J, Pereira C, Fraga S, Fernández J, et al. Moving into advanced nanomaterials. Toxicity of rutile TiO(2) nanoparticles immobilized in nanokaolin nanocomposites on HepG2 cell line. Toxicology and applied pharmacology. 2017;316:114-22; doi: 10.1016/j.taap.2016.12.018.
36. Azqueta A, Dusinska M. The use of the comet assay for the evaluation of the genotoxicity of nanomaterials. Front Genet. 2015;6:239-; doi: 10.3389/fgene.2015.00239.
37. Ferraro D, Anselmi-Tamburini U, Tredici IG, Ricci V, Sommi P. Overestimation of nanoparticles-induced DNA damage determined by the comet assay. Nanotoxicology. 2016;10 7:861-70; doi: 10.3109/17435390.2015.1130274.
38. Di Bucchianico S, Cappellini F, Le Bihanic F, Zhang Y, Dreij K, Karlsson HL. Genotoxicity of TiO2 nanoparticles assessed by mini-gel comet assay and micronucleus scoring with flow cytometry. Mutagenesis. 2017;32 1:127-37; doi: 10.1093/mutage/gew030.
39. Hartmann NB, Jensen KA, Baun A, Rasmussen K, Rauscher H, Tantra R, et al. Techniques and Protocols for Dispersing Nanoparticle Powders in Aqueous Media-Is there a Rationale for Harmonization? Journal of toxicology and environmental health Part B, Critical reviews. 2015;18 6:299-326; doi: 10.1080/10937404.2015.1074969.
40. Jalili P, Gueniche N, Lanceleur R, Burel A, Lavault M-T, Sieg H, et al. Investigation of the in vitro genotoxicity of two rutile TiO2 nanomaterials in human intestinal and hepatic cells and evaluation of their interference with toxicity assays. NanoImpact. 2018;11:69-81; doi: 10.1016/j.impact.2018.02.004.
41. Aninat C, Piton A, Glaise D, Le Charpentier T, Langouët S, Morel F, et al. Expression of cytochromes P450, conjugating enzymes and nuclear receptors in human hepatoma HepaRG cells. Drug

Metabolism and Disposition. 2006;34 1:75; doi: 10.1124/dmd.105.006759.

42. DeLoid GM, Cohen JM, Pyrgiotakis G, Demokritou P. Preparation, characterization, and in vitro dosimetry of dispersed, engineered nanomaterials. Nature protocols. 2017;12 2:355-71; doi: 10.1038/nprot.2016.172.
43. Le Hégarat L, Huet S, Fessard V. A co-culture system of human intestinal Caco-2 cells and lymphoblastoid TK6 cells for investigating the genotoxicity of oral compounds. Mutagenesis. 2012;27 6:631-6; doi: 10.1093/mutage/ges028.
44. Dušinská M, Collins A. Detection of Oxidised Purines and UV-induced Photoproducts in DNA of Single Cells, by Inclusion of Lesion-specific Enzymes in the Comet Assay. Alternatives to Laboratory Animals. 1996;24 3:405-11; doi: 10.1177/026119299602400315.
45. Collins AR, Duthie SJ, Dobson VL. Direct enzymic detection of endogenous oxidative base damage in human lymphocyte DNA. Carcinogenesis. 1993;14 9:1733-5; doi: 10.1093/carcin/14.9.1733.
46. OCDE. Test No. 487: In Vitro Mammalian Cell Micronucleus Test. 2010.
47. Sasaki K, Mizusawa H, Ishidate M. Isolation and characterization of ras-transfected BALB/3T3 clone showing morphological transformation by 12-O-tetradecanoyl-phorbol-13-acetate. Jpn J Cancer Res. 1988;79 8:921-30; doi: 10.1111/j.1349-7006.1988.tb00056.x.
48. OECD. Guidance document on the in vitro Bhas 42 cell transformation assay. Series on Testing & Assessment No. 231. 2017; doi: http://www.oecd.org/officialdocuments/publicdisplaydocumentpdf/?cote=ENV/JM/MONO(2016)1&doclanguage=en.
49. Fontana C, Kirsch A, Seidel C, Marpeaux L, Darne C, Gaté L, et al. In vitro cell transformation induced by synthetic amorphous silica nanoparticles. Mutation research. 2017;823:22-7; doi: 10.1016/j.mrgentox.2017.08.002.
50. Radziun E, Dudkiewicz Wilczynska J, Ksiazek I, Nowak K, Anuszewska EL, Kunicki A, et al. Assessment of the cytotoxicity of aluminium oxide nanoparticles on selected mammalian cells. Toxicology in vitro : an international journal published in association with BIBRA. 2011;25 8:1694-700; doi: 10.1016/j.tiv.2011.07.010.
51. Simon-Deckers A, Gouget B, Mayne-L'Hermite M, Herlin-Boime N, Reynaud C, Carrière M. In vitro investigation of oxide nanoparticle and carbon nanotube toxicity and intracellular accumulation in A549 human pneumocytes. Toxicology. 2008;253 1:137-46; doi: 10.1016/j.tox.2008.09.007.
52. Ivask A, T, Tiina,, V, Meeri, Vija H, K, Aleksandr,, Sihtmae M, et al. Toxicity of 11 Metal Oxide Nanoparticles to Three Mammalian Cell Types In Vitro. Current Topics in Medicinal Chemistry. 2015;15 18:1914-29; doi: 10.2174/1568026615666150506150109.
53. Song Z-M, Tang H, Deng X, Xiang K, Cao A, Liu Y, et al. Comparing Toxicity of Alumina and Zinc Oxide Nanoparticles on the Human Intestinal Epithelium In Vitro Model. Journal of Nanoscience and Nanotechnology. 2017;17 5:2881-91; doi: 10.1166/jnn.2017.13056.
54. Akbaba GB, Turkez H. Investigation of the Genotoxicity of Aluminum Oxide, beta-Tricalcium Phosphate, and Zinc Oxide Nanoparticles In Vitro. International journal of toxicology. 2018;37 3:216-

22; doi: 10.1177/1091581818775709.

55. Gao C-H, Mortimer M, Zhang M, Holden PA, Cai P, Wu S, et al. Impact of metal oxide nanoparticles on in vitro DNA amplification. PeerJ. 2019;7:e7228-e; doi: 10.7717/peerj.7228.
56. Zhang Q, Wang H, Ge C, Duncan J, He K, Adeosun SO, et al. Alumina at 50 and 13 nm nanoparticle sizes have potential genotoxicity. Journal of applied toxicology : JAT. 2017;37 9:1053-64; doi: 10.1002/jat.3456.
57. Yousef MI, Mutar TF, Kamel MAE. Hepato-renal toxicity of oral sub-chronic exposure to aluminum oxide and/or zinc oxide nanoparticles in rats. Toxicology reports. 2019;6:336-46; doi: 10.1016/j.toxrep.2019.04.003.
58. Sliwinska A, Kwiatkowski D, Czarny P, Milczarek J, Toma M, Korycinska A, et al. Genotoxicity and cytotoxicity of ZnO and Al2O3 nanoparticles. Toxicology Mechanisms and Methods. 2015;25 3:176-83; doi: 10.3109/15376516.2015.1006509.
59. Sadiq R, Khan QM, Mobeen A, Hashmat AJ. In vitro toxicological assessment of iron oxide, aluminium oxide and copper nanoparticles in prokaryotic and eukaryotic cell types. Drug and Chemical Toxicology. 2015;38 2:152-61; doi: 10.3109/01480545.2014.919584.
60. Shah SA, Yoon GH, Ahmad A, Ullah F, Amin FU, Kim MO. Nanoscale-alumina induces oxidative stress and accelerates amyloid beta (Aβ) production in ICR female mice. Nanoscale. 2015;7 37:15225-37; doi: 10.1039/C5NR03598H.
61. Li X, Zhang C, Zhang X, Wang S, Meng Q, Wu S, et al. An acetyl-L-carnitine switch on mitochondrial dysfunction and rescue in the metabolomics study on aluminum oxide nanoparticles. Particle and fibre toxicology. 2016;13:4-; doi: 10.1186/s12989-016-0115-y.
62. Hussain SM, Hess KL, Gearhart JM, Geiss KT, Schlager JJ. In vitro toxicity of nanoparticles in BRL 3A rat liver cells. Toxicology in Vitro. 2005;19 7:975-83; doi: 10.1016/j.tiv.2005.06.034.
63. Magdolenova Z, Collins A, Kumar A, Dhawan A, Stone V, Dusinska M. Mechanisms of genotoxicity. A review of in vitro and in vivo studies with engineered nanoparticles. Nanotoxicology. 2014;8 3:233-78; doi: 10.3109/17435390.2013.773464.
64. Karlsson HL, Di Bucchianico S, Collins AR, Dusinska M. Can the comet assay be used reliably to detect nanoparticle-induced genotoxicity? Environmental and molecular mutagenesis. 2015;56 2:82-96; doi: 10.1002/em.21933.
65. Heli H. A study of double stranded DNA adsorption on aluminum surface by means of electrochemical impedance spectroscopy. Colloids and Surfaces B: Biointerfaces. 2014;116:526-30; doi: 10.1016/j.colsurfb.2014.01.046.
66. Zhang R-Y, Liu Y, Pang D-W, Cai R-X, Qi Y-P. Spectroscopic and Voltammetric Study on the Binding of Aluminium(III) to DNA. Analytical Sciences. 2002;18 7:761-6; doi: 10.2116/analsci.18.761.
67. Zhang F, Cao Q, Cheng J, Zhang C, An N, Bi S. Electrochemical and Spectrometric Studies of Double-Strand Calf Thymus Gland DNA Denatured by Al(III) at Neutral pH. Analytical Sciences. 2009;25 8:1019-23; doi: 10.2116/analsci.25.1019.

68. Sakai A, Sasaki K, Muramatsu D, Arai S, Endou N, Kuroda S, et al. A Bhas 42 cell transformation assay on 98 chemicals: The characteristics and performance for the prediction of chemical carcinogenicity. Mutation Research/Genetic Toxicology and Environmental Mutagenesis. 2010;702 1:100-22; doi: 10.1016/j.mrgentox.2010.07.007.
69. Sabella S, Carney RP, Brunetti V, Malvindi MA, Al-Juffali N, Vecchio G, et al. A general mechanism for intracellular toxicity of metal-containing nanoparticles. Nanoscale. 2014;6 12:7052-61; doi: 10.1039/C4NR01234H.
70. Krause B, Meyer T, Sieg H, Kästner C, Reichardt P, Tentschert J, et al. Characterization of aluminum, aluminum oxide and titanium dioxide nanomaterials using a combination of methods for particle surface and size analysis. RSC Advances. 2018;8 26:14377 - 88; doi: 10.1039/c8ra00205c.
71. Harris WR, Berthon G, Day JP, Exley C, Flaten TP, Forbes WF, et al. Speciation of aluminum in biological systems. Journal of Toxicology and Environmental Health. 1996;48 6:543-68; doi: 10.1080/009841096161069.
72. Verstraeten SV, Oteiza PI. Effects of Al3+ and Related Metals on Membrane Phase State and Hydration: Correlation with Lipid Oxidation. Archives of Biochemistry and Biophysics. 2000;375 2:340-6; doi: 10.1006/abbi.1999.1671.
73. Verstraeten SV, Golub MS, Keen CL, Oteiza PI. Myelin Is a Preferential Target of Aluminum-Mediated Oxidative Damage. Archives of Biochemistry and Biophysics. 1997;344 2:289-94; doi: 10.1006/abbi.1997.0146.
74. Villarini M, Gambelunghe A, Giustarini D, Ambrosini MV, Fatigoni C, Rossi R, et al. No evidence of DNA damage by co-exposure to extremely low frequency magnetic fields and aluminum on neuroblastoma cell lines. Mutatation Research. 2017;823:11-21; doi: 10.1016/j.mrgentox.2017.09.001.
75. Hanas JS, Gunn CG. Inhibition of transcription factor IIIA-DNA interactions by xenobiotic metal ions. Nucleic Acids Res. 1996;24 5:924-30; doi: 10.1093/nar/24.5.924.
76. Krause BC, Kriegel FL, Rosenkranz D, Dreiack N, Tentschert J, Jungnickel H, et al. Aluminum and aluminum oxide nanomaterials uptake after oral exposure - a comparative study. Sci Rep. 2020;10 1:2698-; doi: 10.1038/s41598-020-59710-z.

Tables

Table 1: Summary of NM characteristics as reported by the supplier.

NM	NM-code	Average particle sizea (nm)	SSAb (m2/g)	Purity c	Bulk density True densityd (g/cm3)	Morphology
Al0	NM-0015-HP	18	40-60	> 99%	2.70 0.008-0.20	spherical
Al2O3	NM-0036-HP	20	<200	99%	- 0.9	spherical
ZnO	NM-0011-HP	20	50	99.5%	5.6 0.3-0.45	Nearly spherical

a Average particle size was determined by TEM

b Average specific surface area (SSA) was determined by Brunauer-Emmet-Teller (BET)

c Purity was determined by X-ray Powder Diffraction (XRD)

d Density was assessed by normal volumetric test

Table 2: Physico-chemical characterization of Al0, Al2O3 and ZnO NMs.

Sample (100 µg/ml)	PdI	Z-Ave (d.nm)	PdI	Z-Ave (d.nm)
	Dispersion solution (0h)		Dispersion solution (24 h)	
Al0	0.173 ± 0.004	254 ± 4	0.159 ± 0.026	253 ± 12
Al2O3	0.235 ± 0.015	168 ± 3	0.186 ± 0.021	160 ± 2
ZnO	0.104 ± 0.038	233 ± 11	0.112 ± 0.045	189 ± 18
	DMEM 10% FBS (0h)		DMEM 10% FBS (24h)	
Al0	0.176 ± 0.011	197 ± 2	0.156 ± 0.011	201 ± 1
Al2O3	0.521 ± 0.027	81 ± 1	0.337 ± 0.041	108 ± 1
ZnO	0.262 ± 0.010	198 ± 4	0.178 ± 0.019	156 ± 9
	William's 5% FBS (0h)		William's 5% FBS (24h)	
Al0	0.158 ± 0.008	240 ± 14	0.152 ± 0.007	246 ± 12
Al2O3	0.466 ± 0.015	107 ± 2	0.442 ± 0.018	120 ± 2
ZnO	0.233 ± 0.030	208 ± 6	0.165 ± 0.011	182 ± 11

The mean hydrodynamic diameter (z-Ave) and polydispersity index (PdI) were determined in the stock dispersion solution and cell media (DMEM + 10 % FBS and William's + 5 % FBS) after 0 h and 24 h at a concentration of 100 µg/ml. Three independent experiments were performed. Results are expressed as mean ± SD.

Table 3: Ion release from Al0, Al2O3, ZnO NMs and AlCl3.

NMs	NM concentration (µg/mL)	Dispersion stock solution [%]	DMEM + 10% FBS [%]	William's + 5% FBS [%]
Al0	25	1.30 ± 0.06	3.88 ± 0.13	2.42 ± 0.07
	50	0.85 ± 0.05	1.94 ± 0.09	1.26 ± 0.07
	100	0.48 ± 0.02	0.95 ± 0.04	0.68 ± 0.01
Al2O3	25	0.24 ± 0.04	0.40 ± 0.03	0.32 ± 0.11
	50	0.18 ± 0.08	0.48 ± 0.06	0.35 ± 0.07
	100	0.15 ± 0.01	0.37 ± 0.02	0.27 ± 0.02
AlCl3	25	89.60 ± 5.97	57.16 ± 5.97	23.35 ± 0.26
	50	81.72 ± 0.77	30.09 ± 0.44	12.86 ± 0.28
	100	94.31 ± 6.61	17.54 ± 0.72	6.47 ± 0.52
ZnO	25	29.21 ± 0.53	85.09 ± 5.30	54.99 ± 1.03
	50	15.07 ± 0.10	57.97 ± 0.68	28.54 ± 1.18
	100	7.40 ± 0.05	30.21 ± 0.23	14.74 ± 0.21

Ion release was determined by ICP-MS in the stock dispersion solution and the cell media (DMEM + 10 % FBS and William's + 5 % FBS) after 24 h at concentrations of 25, 50 or 100 µg/mL. Data are presented as the mean ± SD of three independent experiments.

Table 4: Detection of chromosomal damage in differentiated Caco-2 and HepaRG cells treated with Al-containing NMs.

		Caco2		HepaRG	
		%BNMN	RI (%)	% BNMN	RI (%)
Control	0	5.6 ± 0.3	100 ± 0	3.6 ± 0.5	100 ± 0
Al0 NMs	3	5.7 ± 0.4	97 ± 0.8	3.2 ± 0.3	97 ± 5.7
[µg/cm2]	9	5.7 ± 0.5	99 ± 3	3.2 ± 0.2	99 ± 3.1
	28	5.5 ± 0.4	103 ± 3.3	2.4 ± 0.2	101 ± 6.7
	40	5.9 ± 0.6	98 ± 2.6	3.5 ± 0.9	101 ± 5.5
	80	6 ± 0.5	94 ± 0.6	2.2 ± 0.3	110 ± 4.5
Al2O3 NMs	3	6.4 ± 1	102 ± 4	3.6 ± 0.6	99 ± 3.3
[µg/cm2]	9	5.6 ± 1.4	100 ± 2.9	3.3 ± 0.3	102 ± 5.2
	28	6.3 ± 1.4	96 ± 2.2	4.5 ± 0.8	109 ± 7.2
	40	6.4 ± 0.7	98 ± 0.7	3.5 ± 0.5	106 ± 6.8
	80	6.4 ± 1	102 ± 4	3.6 ± 0.6	99 ± 3.3
AlCl3	28	6.9 ± 0.5	103 ± 1.5	4.7 ± 1.5	114 ± 3.8
[µg/ml]	40	6.9 ± 0.8	100 ± 1	4.3 ± 0.8	113 ± 3.3
ZnO NMs	3	7 ± 0.8	100 ± 4.1	3.7 ± 0.4	96 ± 3.5
[µg/cm2]	6	8 ± 0.7	96 ± 3.8	4.1 ± 0.4	90 ± 3.4
MMS [µg/mL]		12.4 ± 0.6 **	39 ± 5.7 **	11.2 ± 2.4 **	96 ± 4.9

Cells were treated with increasing concentrations of Al0, Al2O3 and ZnO NMs, and with the ionic salt control AlCl3. MMS was used as a positive control (25 µg/ml for Caco-2 cells and 30 µg/ml for HepaRG cells). Results are presented as means (±SEM) of the percentage of binucleated micronucleated cells (BNMN) scored from 1000 binucleated cells per slide. Two slides per concentration were scored per experiment. Viability was calculated by the replicative index (RI). Each concentration was tested in duplicate, *n*= 3. The percentages of BNMN cells were compared using the one-way Pearson chi-square test.***p<0.01.

Table 5: Effects of Al-containing NMs on cell growth and foci numbers in the CTA assay in Bhas-42 cells. Cells were treated from day 1 to 4 (initiation assay) or from day 4 to 14 (promotion assay) with Al0 and Al2O3 NMs, and with AlC13 and post-cultivated in fresh medium until Day 21. MCA (1 µg/mL) and TPA (0.05 µg/ml) were included as positive controls. The mean of the cell growth (CG) and the number of

transformed foci per well (foci/well) were measured from 3 and 6 replicate cultures respectively, according to the OECD.

		Initiation assay		Promotion assay	
Chemical	Concentration	CG a	Foci/well b	CG a	Foci/well b
Al	0 c (0.005% BSA)	100	5.3 ± 1.5	100	8.7 ± 3.1
	0.03 µg/cm2	107	6.5 ± 1.4	99	4.7 ± 2.1 *
	0.1 µg/cm2	105	5.3 ± 2.4	97	0.7 ± 0.8 *
	0.3 µg/cm2	96	4.2 ± 0.8	89	0.7 ± 0.8 *
	1 µg/cm2	62	2.7 ± 1.6 *	83	Toxic d
	3 µg/cm2	14	1.5 ± 0.8 *	75	Toxic d
Al2O3	0 c (0.005% BSA)	100	5.3 ± 1.5	100	8.7 ± 3.1
	0.3 µg/cm2	106	3.0 ± 2.0 *	103	5.7 ± 2.0 *
	1 µg/cm2	94	3.3 ± 1.5 *	95	7.0 ± 1.3
	3 µg/cm2	97	3.8 ± 0.8	93	5.8 ± 1.6 *
	9 µg/cm2	74	3.5 ± 1.9	83	4.0 ± 1.5 *
	28 µg/cm2	72	2.3 ± 1.6 *	84	0.7 ± 0.5 *
AlCl3	0 c (2.5% H2O)	100	4.7 ± 1.6	100	6.8 ± 1. 7
	3 µg/ml	96	4.7 ± 1.0	96	Toxic d
	9 µg/ml	78	4.3 ± 2.4	88	Toxic d
	28 µg/ml	16	4.0 ± 1.3	80	Toxic d
MCA	0 c (0.1% DMSO)	100	5.8 ± 1.9		
	1 µg/ml	17	14.7 ± 2.9 ≠		
TPA	0 c (0.1% DMSO)			100	8.8 ± 2.1
	0.05 µg/ml			112	20.3 ± 3.0 ≠

a % of cell growth compared to that of vehicle control.

b Average number of transformed foci/well ± SD.

c Vehicle control: final vehicle concentration of the working culture media in parentheses.

d Absence of cells in well.

* $p < 0.05$; Dunnett test, *vs* vehicle control.

≠ $p < 0.05$; *t*-test, *vs* DMSO (the vehicle of MCA and TPA).

Figures

Figure 1

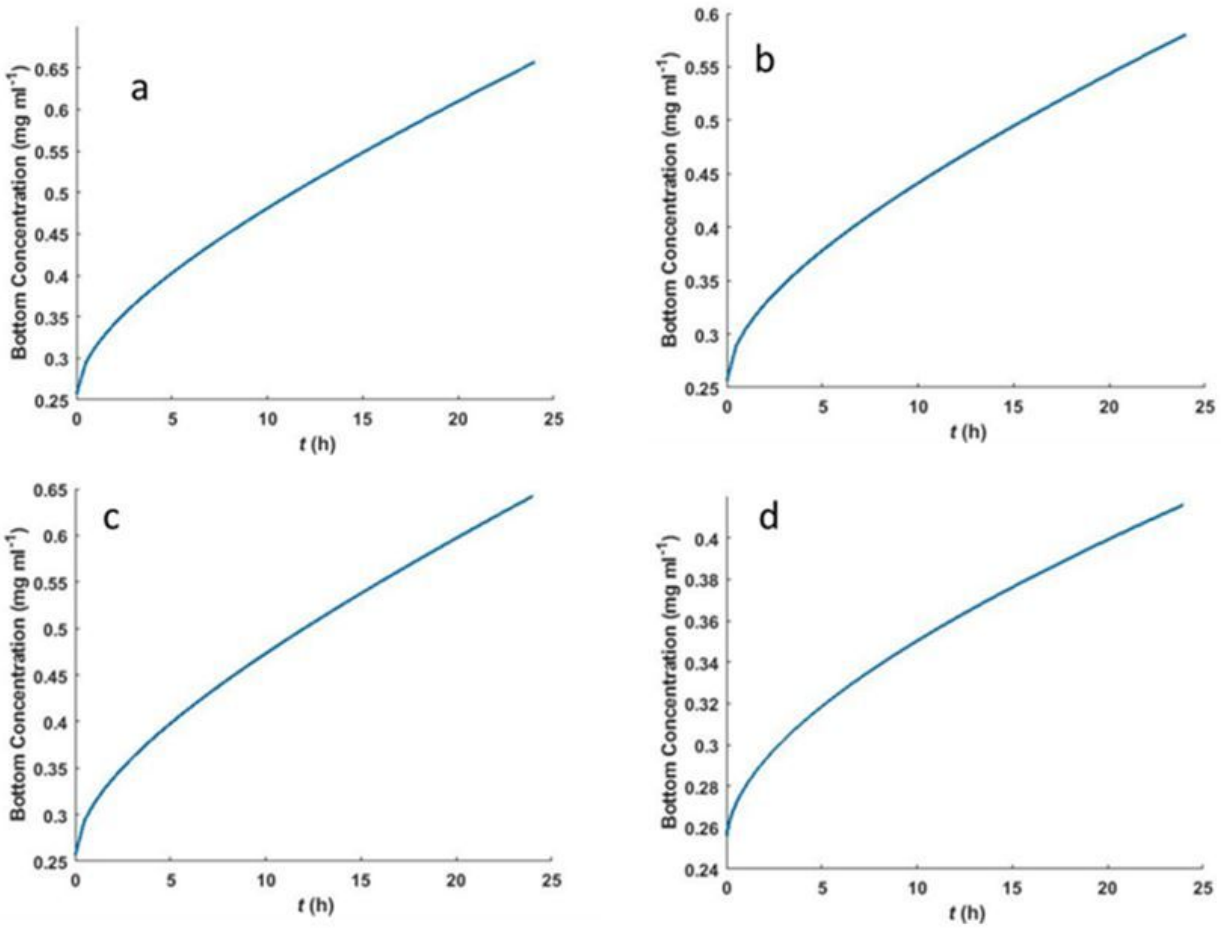

Figure 1

Time evolution over 24 h of the well-bottom concentration of (a) Al0 NMs in DMEM; (b) Al2O3 NMs in DMEM; (c) Al0 NMs in William's medium; (d) Al2O3 NMs in William's medium. Model parameters : bulk NM concentration 250 µg.mL-1; T=37°C.

Figure 2

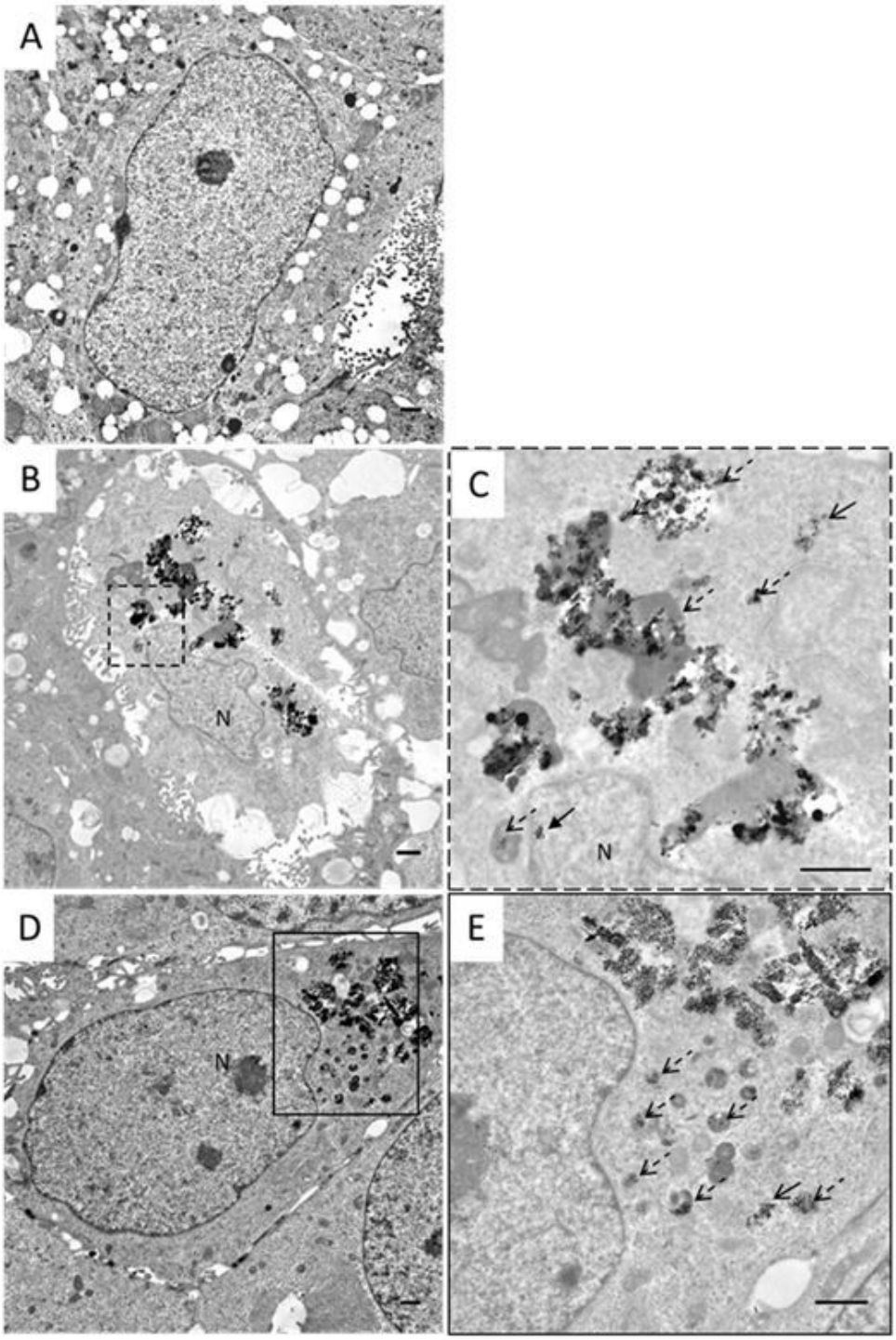

Figure 2

TEM images of differentiated Caco-2 cross-sections showing the uptake of Al0 NMs (B, C) at 21 µg/cm2 and Al2O3 NMs (D,E) at 39 µg/cm2, after 24 h treatment compared to the negative control (A). Concentrations of 21 µg/cm2 Al0 NMs and 39 µg/cm2 Al2O3 NMs were used to ensure equivalent Al content per well. C and E represent enlarged pictures from B and D respectively. C: Al0 NMs were rarely

seen in proximity to the nucleus (full arrow). C, E: NMs are present either in small clusters in the cytoplasm or near the nucleus (open arrow) either as large agglomerates integrated into lucent or dense vesicles (notched arrows). Scale bar 1µm, C: Cytoplasm, N: nucleus.

Figure 3

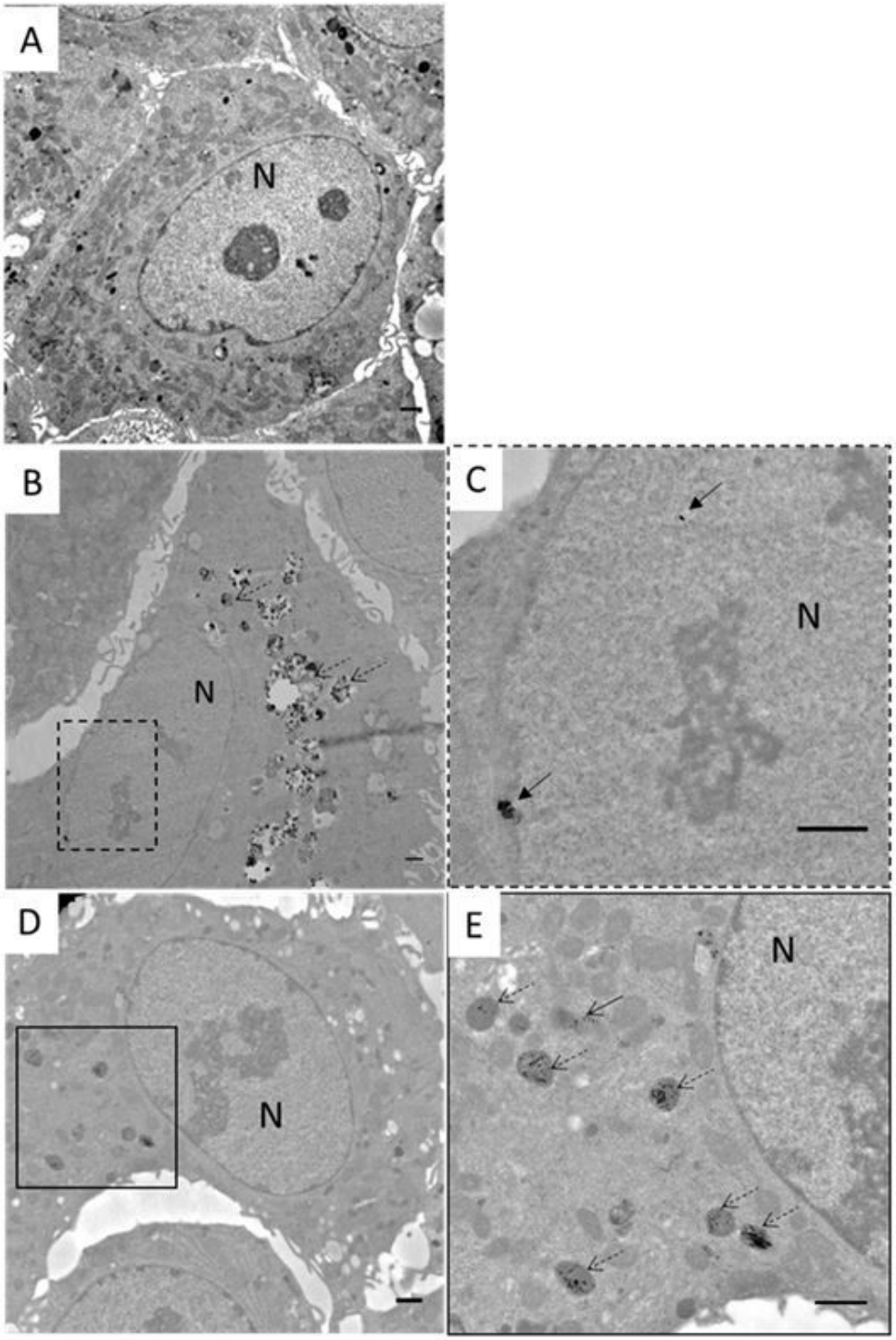

Figure 3

TEM images of differentiated HepaRG cross sections showing the uptake of Al0 (B, C) at 21 µg/cm2 and Al2O3 (D,E) at 39 µg/cm2, after 24 h cell treatment compared to the negative control (A). Concentrations of 21 µg/cm2 Al0 NMs and 39 µg/cm2 Al2O3 NMs were used to ensure equivalent Al content per well. C and E represent enlarged pictures from B and D respectively. C: Al0 NMs were rarely seen near the nucleus

(full arrow). E: NMs are included in vesicles containing large agglomerates (notched arrows) or as dense vesicles containing small clusters in the cytoplasm (open arrow) or as isolated clusters. Scale bar 1µm, C: Cytoplasm, N: nucleus.

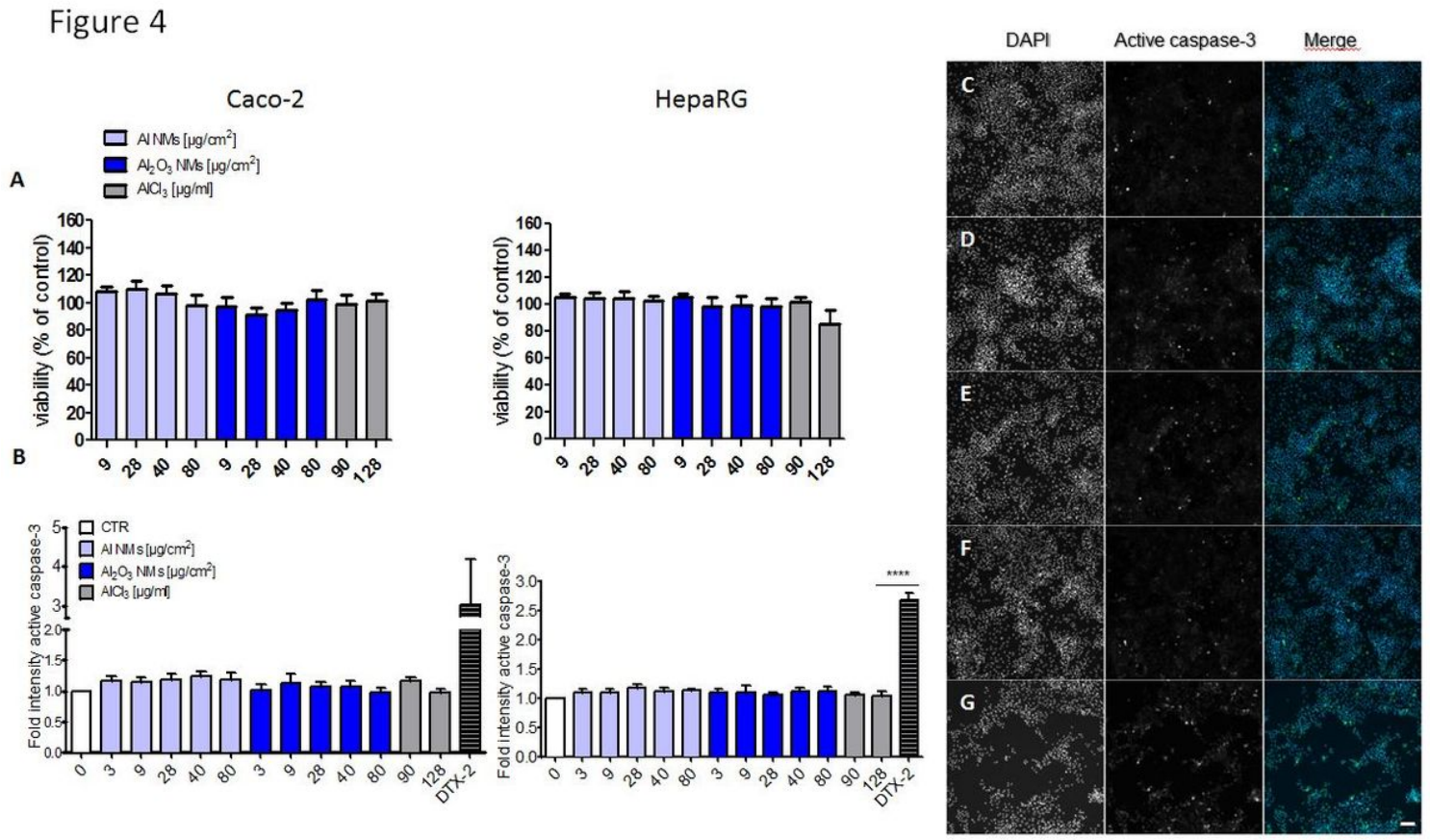

Figure 4

Effects of Al-containing NMs on cell numbers and active caspase-3 levels in differentiated Caco-2 and HepaRG cells. Cells were treated for 24 h with Al0 NMs, Al2O3 NMs and AlCl3 as ionic salt control. ZnO and DTX-2 (20 nM for Caco-2 cells, 15 nM for HepaRG) were used as positive controls. Cell numbers (A) and active-caspase-3 (B) from automated image analysis are presented as fold changes relative to untreated cells. Representative images of active caspase-3 (green) in the cytoplasm of HepaRG cells are shown. C) negative control, D) Al0 NMs 80 µg/cm2, E) Al2O3 NMs 80 µg/cm2, F) AlCl3 128 µg/ml, G) ZnO NMs 6 µg/cm2. Data are presented as the means ± SEM of 3 (Caco-2) or 4 (HepaRG) independent experiments. ****p< 0.0001. White bar = 100 µm

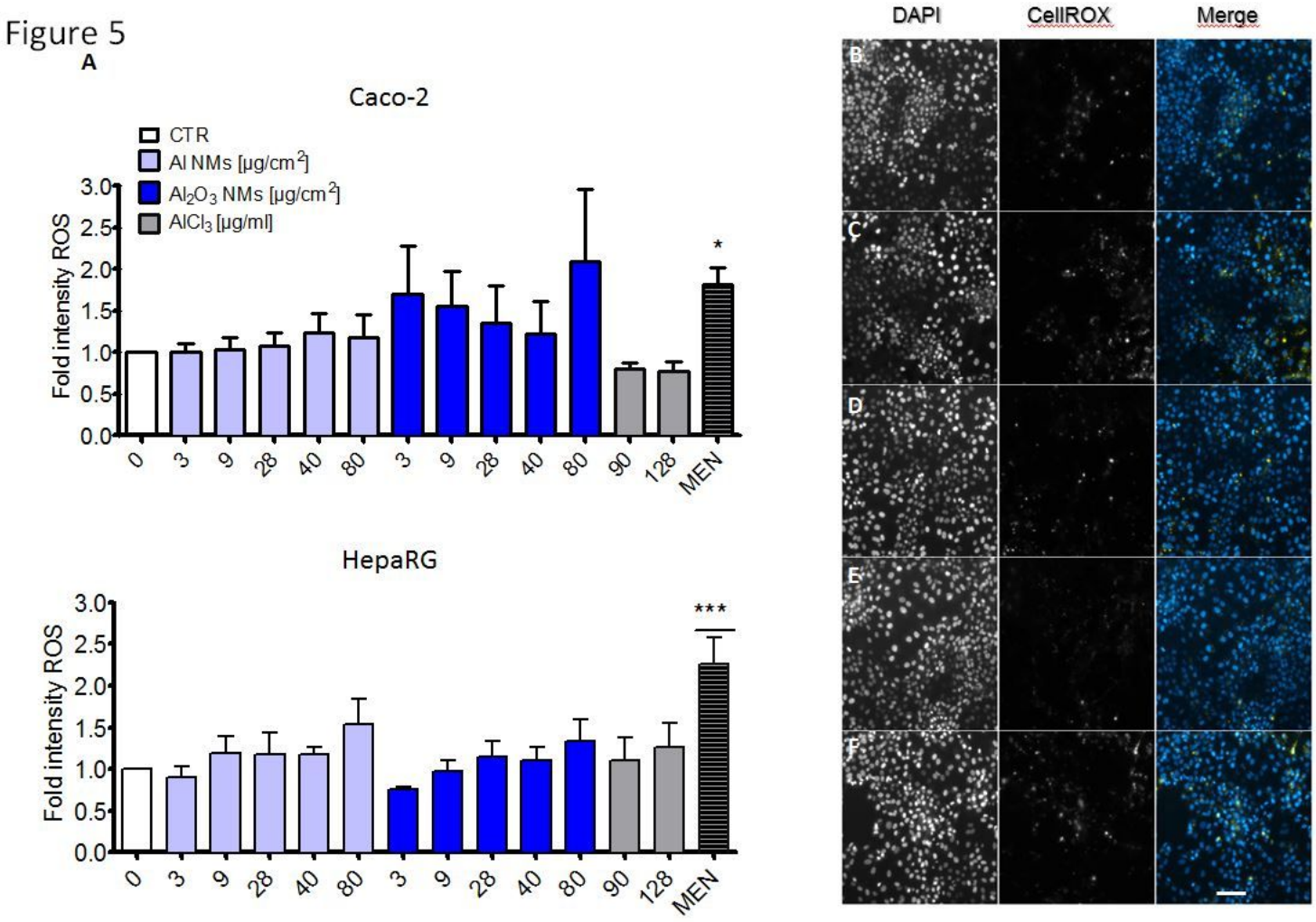

Figure 5

Effects of Al-containing NMs on ROS levels in differentiated Caco-2 and HepaRG cells. A) Cells were treated for 24 h with Al0 NMs, Al2O3 NMs and AlCl3 as ionic salt control. ZnO and Menadione (MEN) (25 µM for HepaRG, 50 µM for Caco-2 cells) were used as positive controls. Representative images of ROS detection (yellow) in the cytoplasm of HepaRG cells are shown. B) negative control, C) Al0 NMs 80 µg/cm2, D) Al2O3 NMs 80 µg/cm2, E) AlCl3 (128 µg/ml), F) ZnO NMs 6 µg/cm2. Data are presented as the means ± SEM of 5 (Caco-2) or 6 (HepaRG) independent experiments. *p< 0.05, ***p<0.001. White bar = 100 µm.

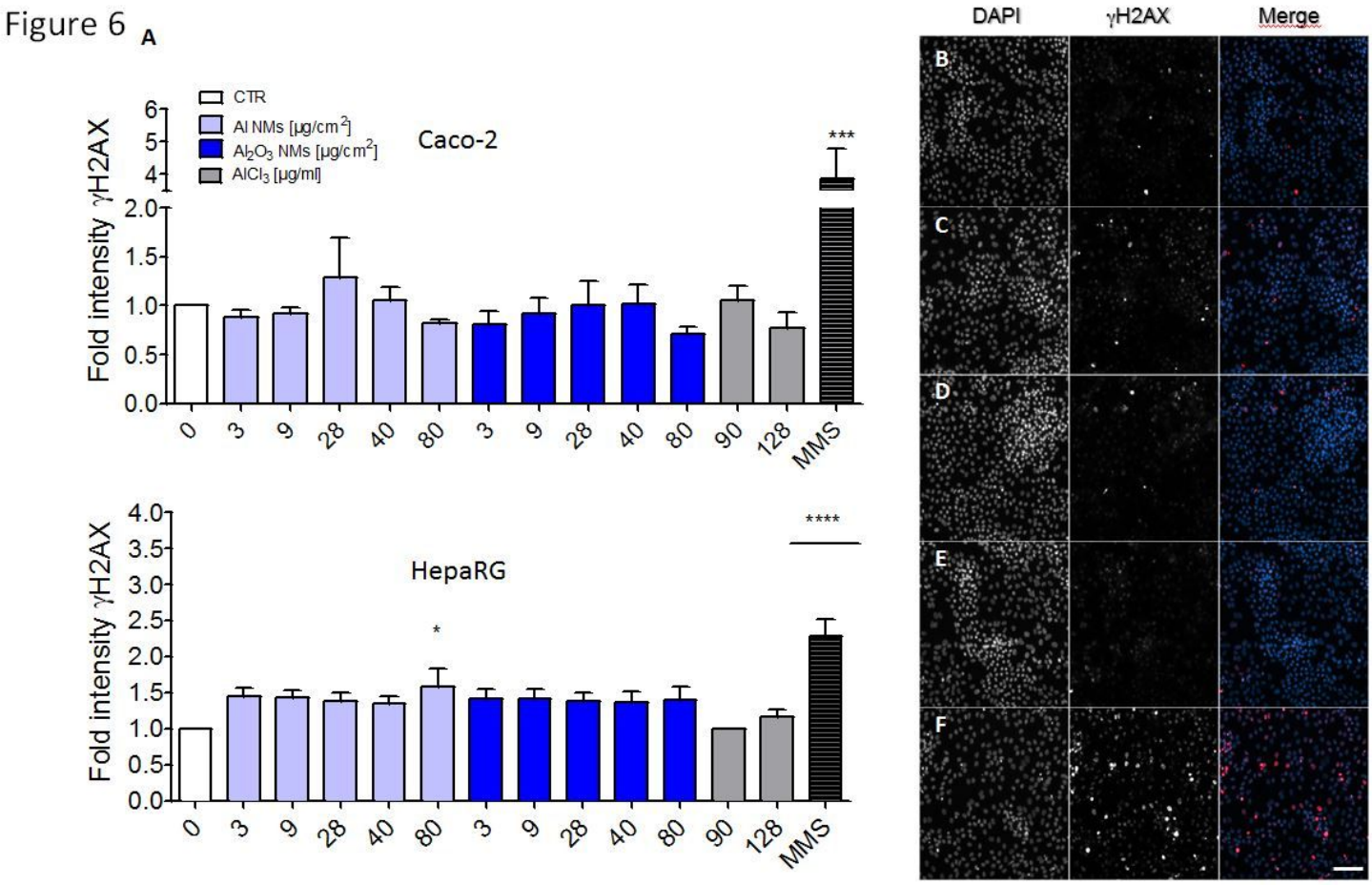

Figure 6

Effects of Al-containing NMs on γH2AX level in Caco-2 and HepaRG Cells. A) Cells were treated for 24 h with Al0 NMs, Al2O3 NMs and AlCl3 as ionic salt control, or positive controls (MMS at 60 or 30 µg/ml respectively, and ZnO NMs). Representative images of γH2AX detection (red) in the nuclei of HepaRG cells: B) negative control, C) Al0 NMs 80 µg/cm2, D) Al2O3 NMs 80 µg/cm2, E) AlCl3 128 µg/ml, F) ZnO NMs 6 µg/cm2. Data are presented as the mean ± SEM of 3 independent experiments. *p< 0.05, ***p<0.001, ****p<0.0001. White bar=100 µm.

Figure 7

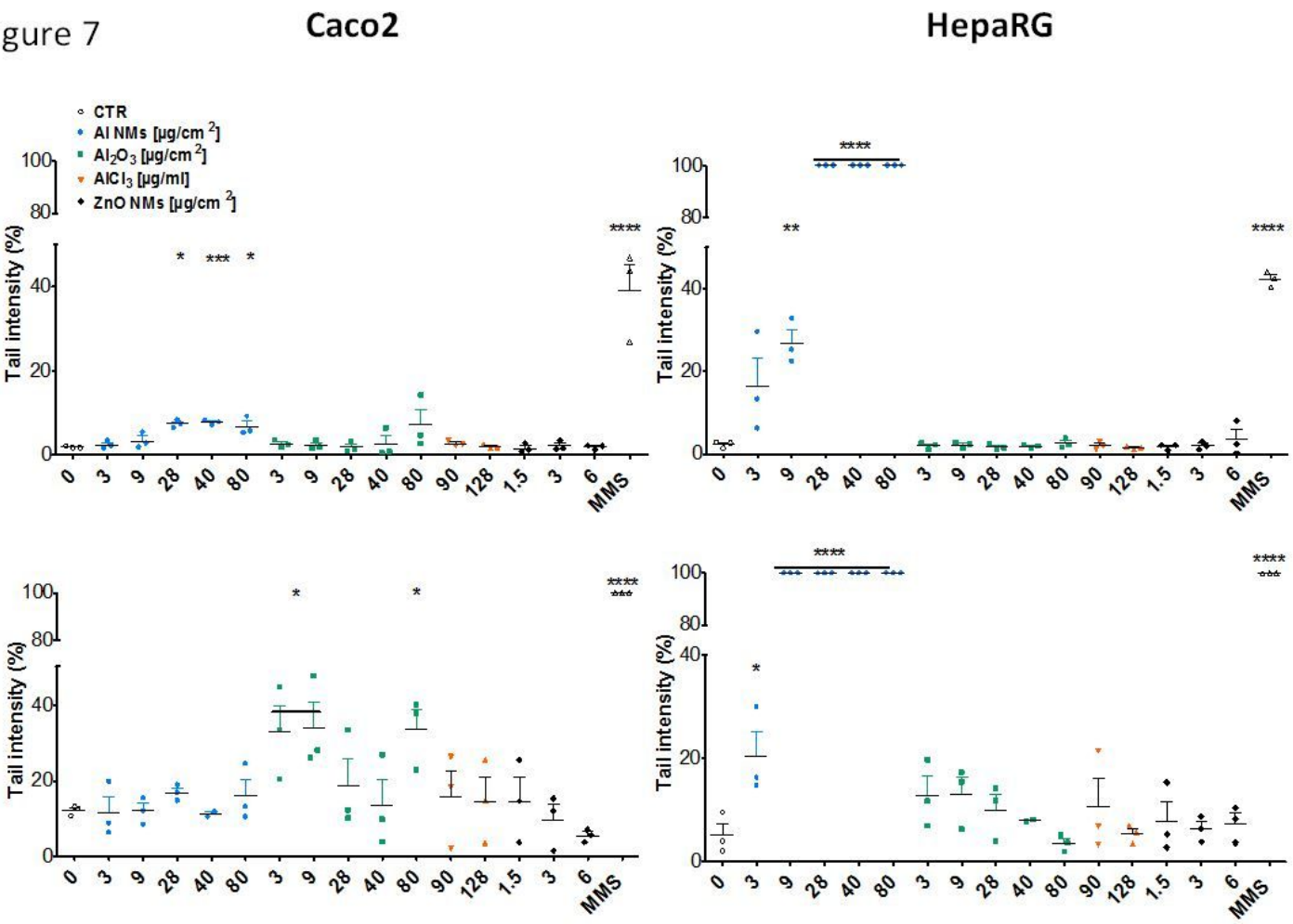

Figure 7

Detection of DNA damage in differentiated Caco-2 and HepaRG cells treated 24 h with Al-containing NMs with the alkaline and Fpg-modified comet assays. DNA damage (A, B) and oxidative DNA damage (C, D) were assessed in differentiated Caco-2 and HepaRG cells treated for 24 h with Al0, Al2O3 and ZnO NMs, and with the ionic salt control AlCl3. MMS was used as a positive control (30 µg/ml). Values are presented as the mean percentage ± SEM of 3 independent experiments. *p < 0.05, **p < 0.01, ***p<0.001, ****p<0.0001.

Figure 8

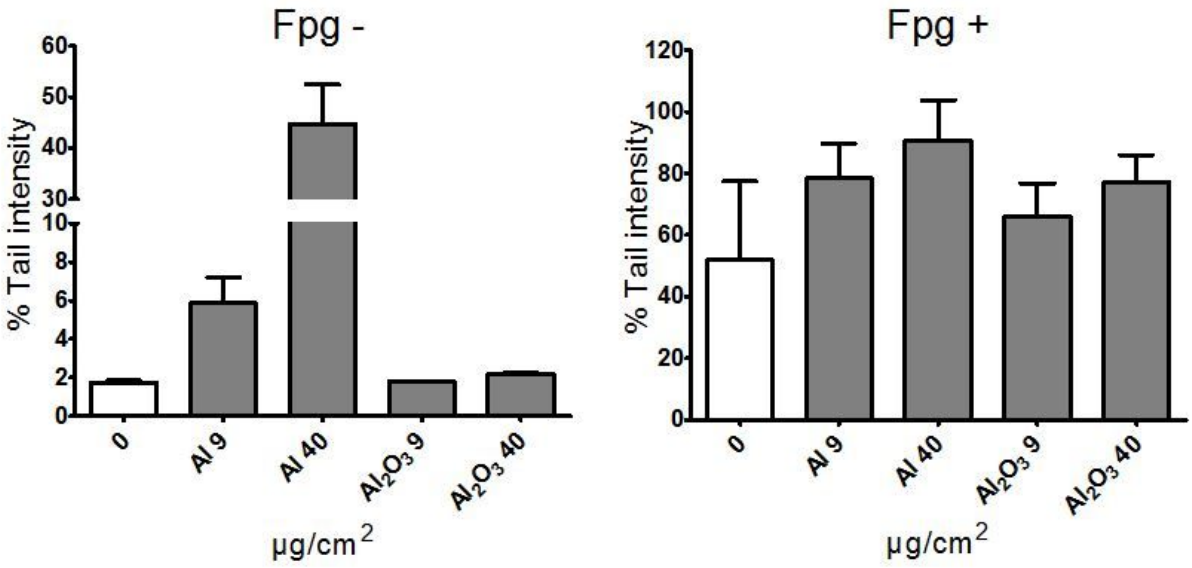

Figure 8

Interference of Al0 and Al2O3 NMs with the alkaline and Fpg-modified comet assays. The interference of Al0 and Al2O3 NMs with DNA migration was assessed with untreated HepaRG cells. NMs were added in LMP when cells are deposited on slides and compared with control (cells without addition of NMs. Values are presented as the mean percentage ± SEM of 2 independent experiments.

Supplementary Files

This is a list of supplementary files associated with this preprint. Click to download.

- SuppdatPFT.ppt